INHERITANCE LOGO

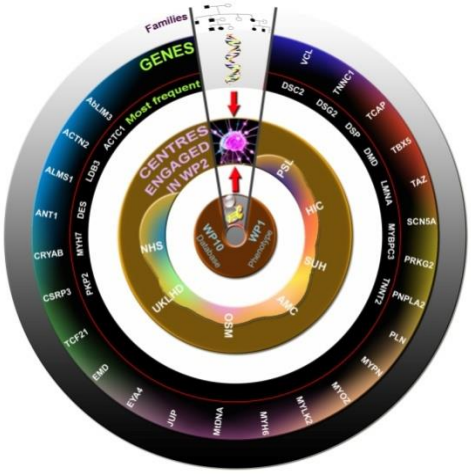

WP1 Phenotypes of DCM subtypes

Figure.1.1

Kaplan-Meier Event-Free Survival From Date of First Visit to Cardiologist Kaplan-Meier event-free survival stratified by 3 independent risk factors (RF): nonsustained ventricular tachycardia, left ventricular ejection fraction <45% at the first visit to the cardiologist, and being male. Event: occurrence of malignant ventricular arrhythmias, defined as appropriate implantable cardioverter-defibrillator treatment, cardiopulmonary resuscitation, or sudden cardiac death.	Kaplan-Meier Event-Free Survival All 4 Risk Factors Kaplan-Meier event-free survival stratified by 4 independent risk factors (RF): nonsustained ventricular tachycardia, left ventricular ejection fraction <45% at the first visit to the cardiologist, being male, and non-missense mutations (ins-del/truncating or mutations affecting splicing). Event: occurrence of malignant ventricular arrhythmias, defined as appropriate implantable cardioverter-defibrillator treatment, cardiopulmonary resuscitation, or sudden cardiac death.
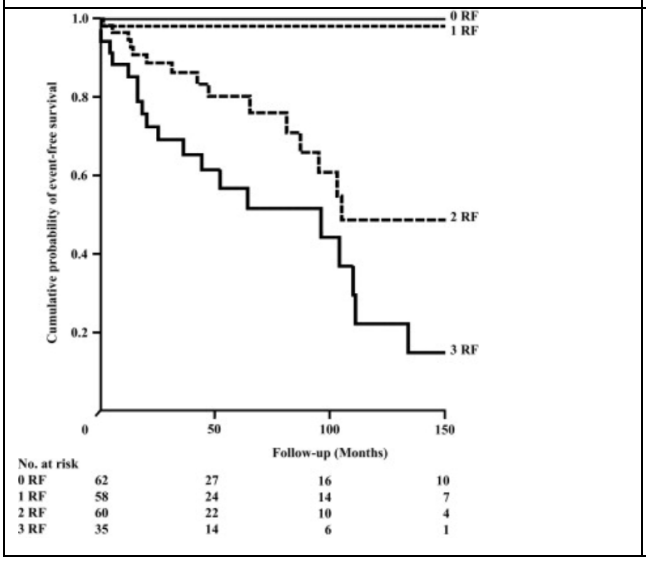	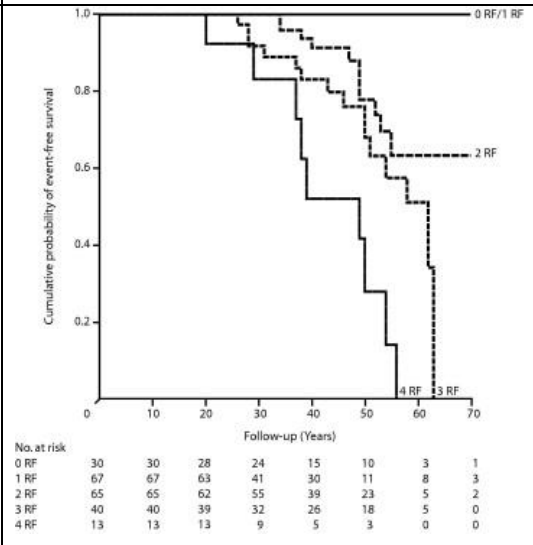

Figure. 1.2

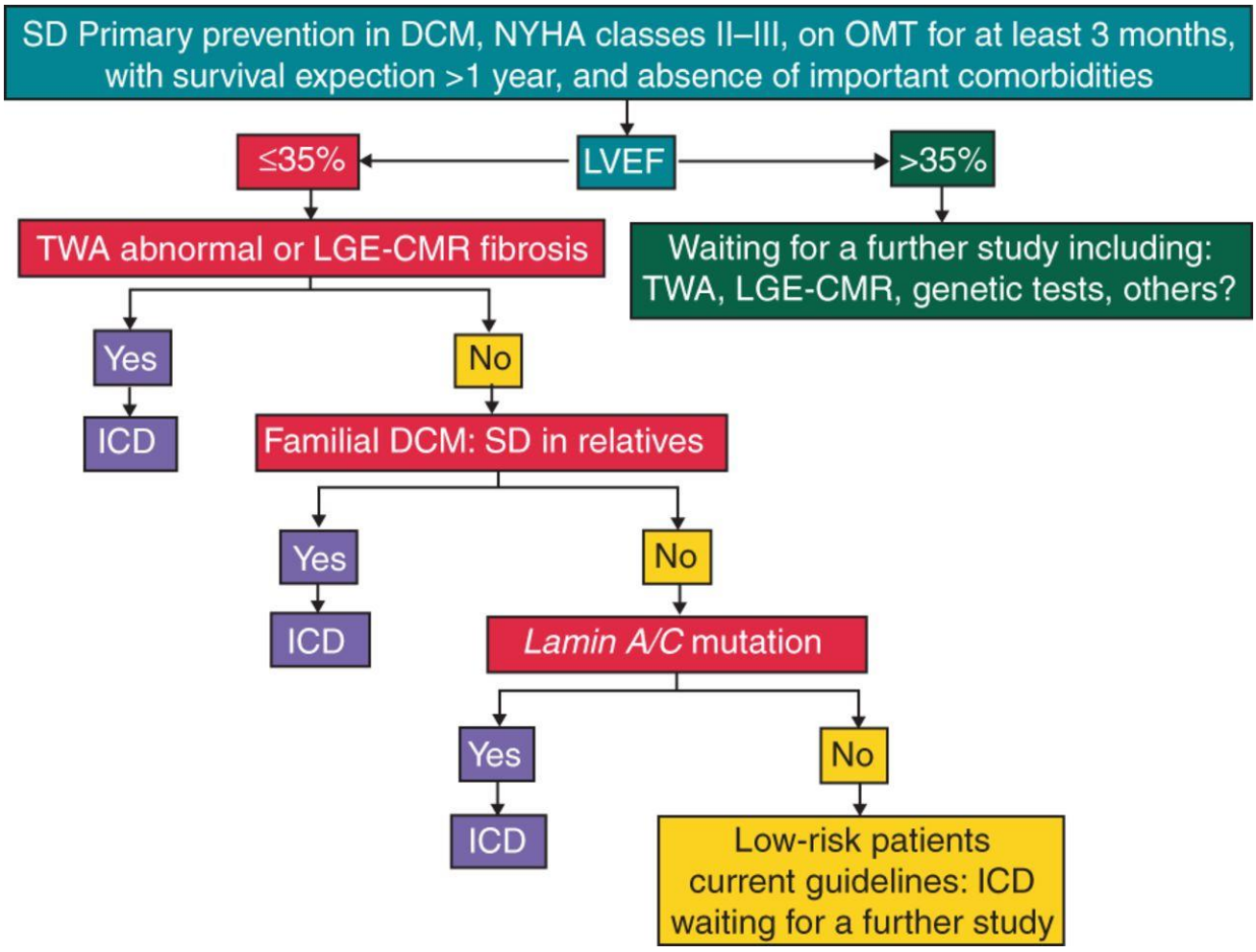
SD Primary prevention in DCM, NYHA classes II–III, on OMT for at least 3 months, with survival expection >1 year, and absence of important comorbidities
LVEF
≤35%
>35%
TWA abnormal or LGE-CMR fibrosis
Waiting for a further study including: TWA, LGE-CMR, genetic tests, others?
Yes
No
ICD
Familial DCM: SD in relatives
Yes
No
ICD
Lamin A/C mutation
Yes
No
ICD
Low-risk patients current guidelines: ICD waiting for a further study

Figure 1.3

Kaplan-Meier Event-Free Survival and Cum Inc for Competing Events Kaplan-Meier event-free survival curve for the combined event of death and heart transplantation (HTx). The number of patients at risk is reported at the bottom of the figure immediately above the x-axis.	Kaplan-Meier Event-Free Survival and Cum Inc for Competing Events Cumulative incidence (Cum Inc) for the competing events of death and HTx. Cumulative incidence (Cum Inc) (95% confidence interval [CI]) at the end of the follow-up is reported for each outcome.
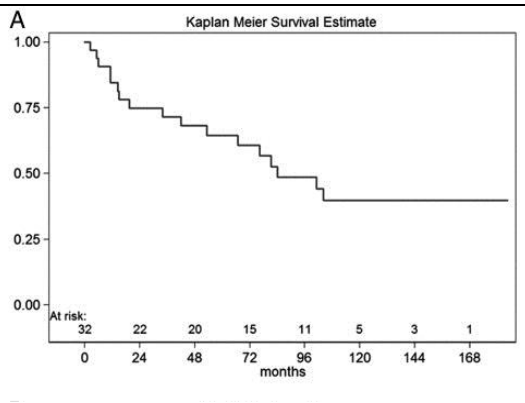	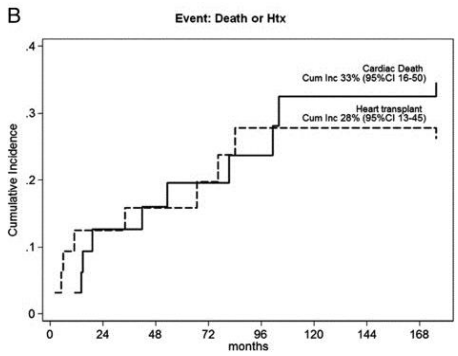

Figure. 1.4

App at
http://moges.biomeris.com

$M_{H}\ O_{H}\ G_{AD}\ E_{G\text{-}MYH7[R663H]}\ S_{B\text{-}I}$

Relatives:

$M_{E[H]}\ O_{H}\ G_{AD}\ E_{G\text{-}MYH7[R663H]}\ S_{A\text{-}I}$

$M_{0(H)}\ O_{H}\ G_{AD}\ E_{G\text{-}MYH7[R663H]}\ S_{A\text{-}I}$

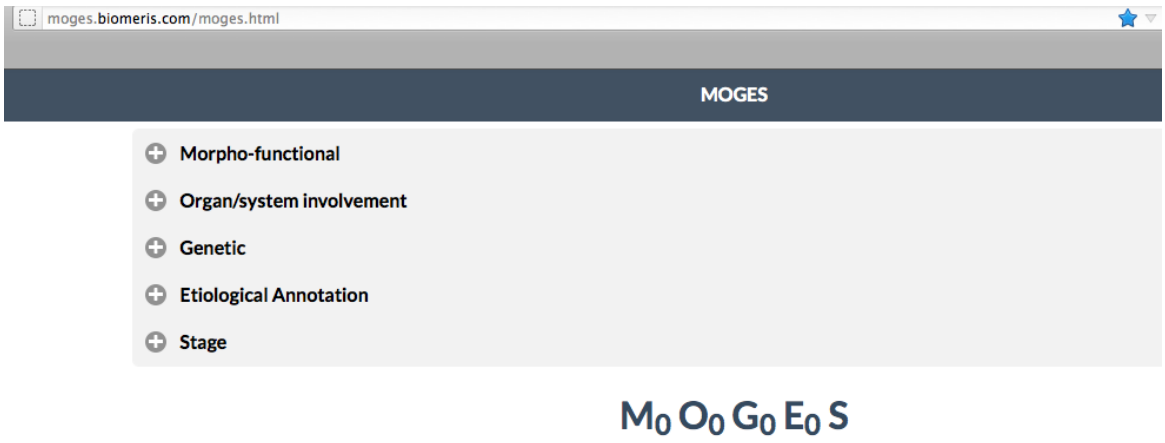

$M_0\ O_0\ G_0\ E_0\ S$

WP2 Genetic testing

Figure. 2.1

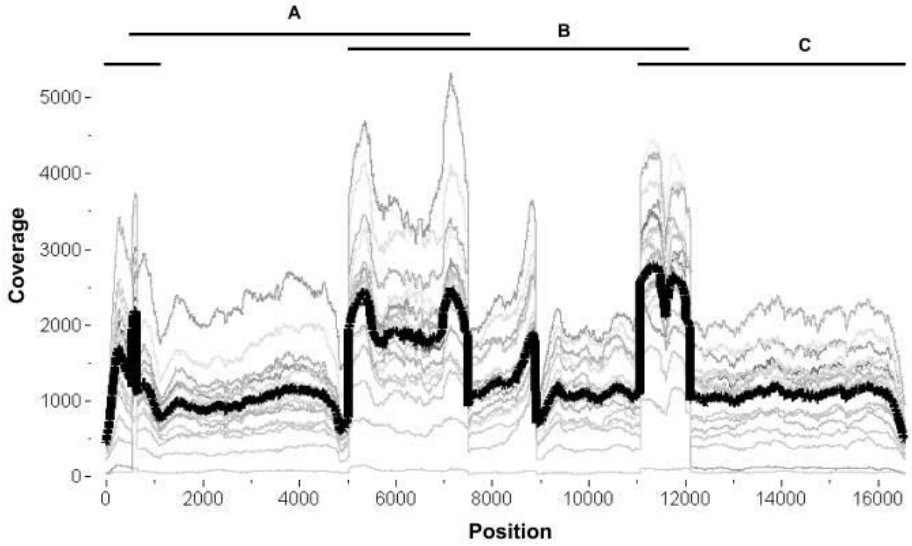

Figure. 2.1 : Variability in 454 sequence coverage. Total read coverage (redundant and non-redundant) is plotted at each mtDNA position (1 to 16569) and graphed as a continuous thin grey trace for each case (different shades for each case). The mean coverage for all 20 cases is represented by a thick dark black trace. The shape of the traces shows coverage variability both between cases and along the same mtDNA. The black horizontal lines (A, B & C) above the graph represent the three mtDNA PCR fragments used for 454 sequencing. Greater coverage was noted in the regions in which the PCR fragments overlap compared to coverage in non-overlapping regions.

Figure. 2.2

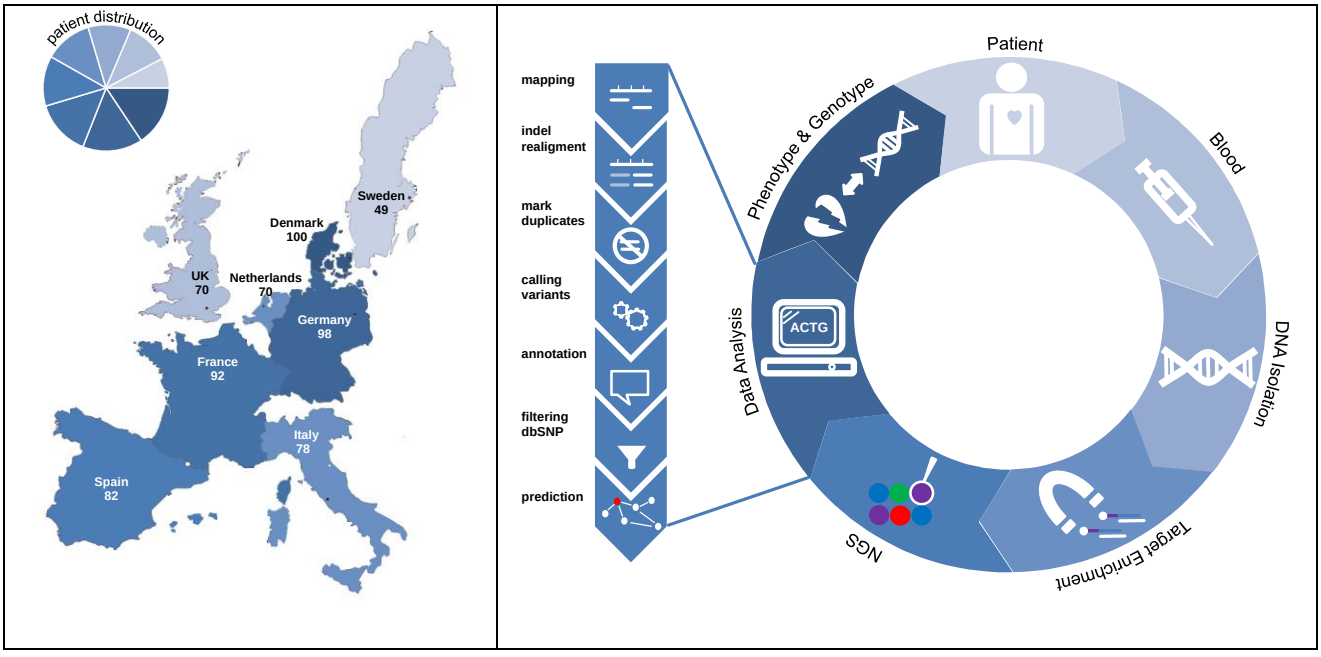

Figure. 2.2: The NGS plan in INHERITANCE.

Figure.2.3

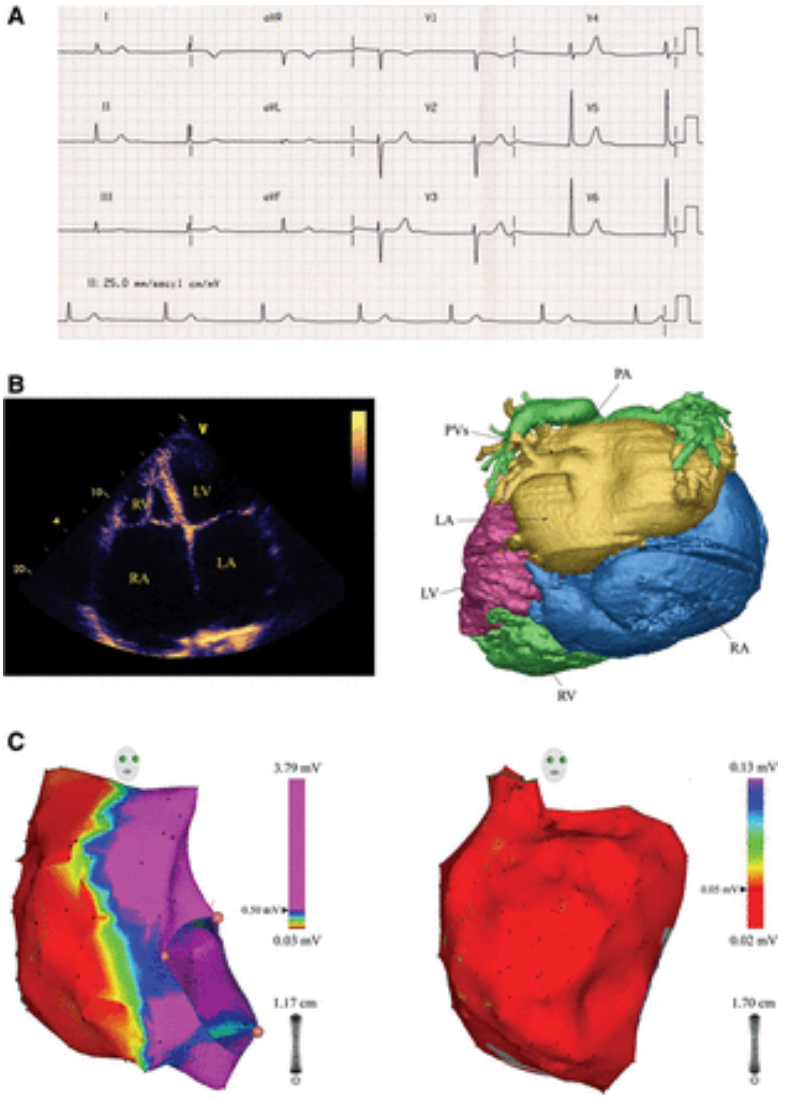

Figure 2.3: The figure shows the key phenotypical traits of the novel cardiomyopathy. (A) Surface ECG with complete atrial standstill: bradycardic (39 bpm) junctional rhythm without atrial activity and narrow QRS (patient A:V:1). (B) Giant atria are shown by ultrasound examination and by 3-dimensional cardiac tomography (3DCT) imaging. On the left, the apical 4-chamber view of the patient A:IV:5. On the right, 3DCT reconstruction of the cardiac chambers24 of patient A:V:1. Colours inner surfaces of the districts are shown in right posterior view. Right atrial (RA) and left atrial (LA) volumes are 744 and 426 mL, respectively; left (LV) and right ventricular (RV) volumes are 138 mL and 252 mL, respectively (see online-only Data Supplement Video). Pulmonary arteries (PA) and pulmonary veins (PVs) are shown at the top. (C) Scars in the RA are shown by 3D voltage mapping (right anterior projection) in patients D:IV:2 (at the left) and A:V:1 (at the right) with Brady–Tachy syndrome and complete atrial standstill, respectively. In the

former, the scar is localized at lateral wall, whereas in the latter, the scar is diffused (red colour indicates voltages <0.05 mV).

WP3 Genome-wide association studies

Figure 3.1 - GWAS Paris

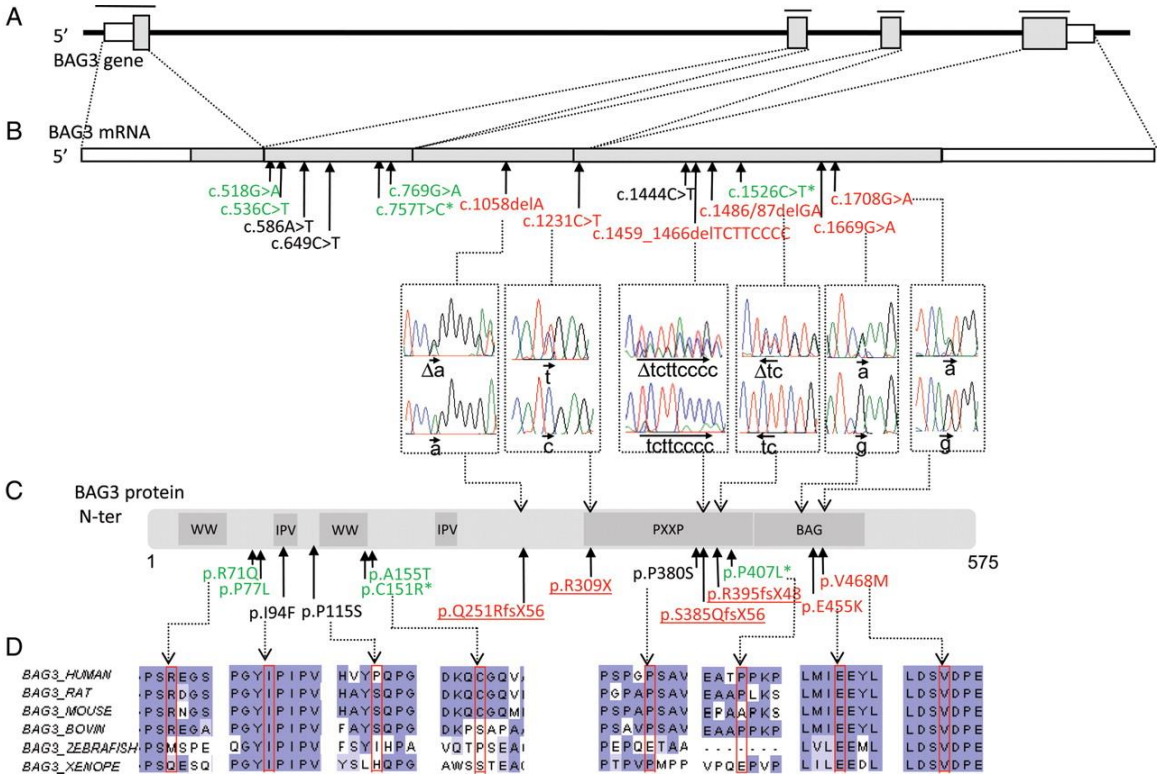

Figure 3.1: Variants in BAG3 found in index patients with familial dilated cardiomyopathy (DCM). (A) Genomic structure of the BAG3 gene. The four exons are presented as boxes (white for UTR, grey for coding). Upper horizontal lines indicate sequenced regions. (B) BAG3 transcript with all missense and frame shift variants positions identified in familial DCM cases indicated. The variants are classified as likely disease causing (red), possibly disease causing (black), or probably neutral (green) as explained in the Results section. *Indicates SNPs associated with sporadic DCM in the GWAS. All likely and possibly disease-causing variants were found each in a single independent individual at the heterozygous state. The electrophoregrams representative of heterozygous mutated (upper) and homozygous wild-type (lower) sequences are shown for each DCM mutation. The arrows indicate the modified nucleotides and the sequenced strand orientation. (C) Schematic representation of the BAG3 protein with referenced domain signature according to UniprotKB database38 and dark grey boxes. The consequences of the DNA variants in (B) are shown as resultant predicted amino acid changes with the same colour code. (D) The ClustalW multiple alignments of orthologous BAG3 sequences from different species restricted to the immediate

vicinity of each missense variant (red boxes) with MAF > 5% is shown. Interspecies conservation is indicated as blue boxes (dark blue: identical; light blue: similar; white: not conserved amino acid).

Figure 3.2 – GWAS Heidelberg

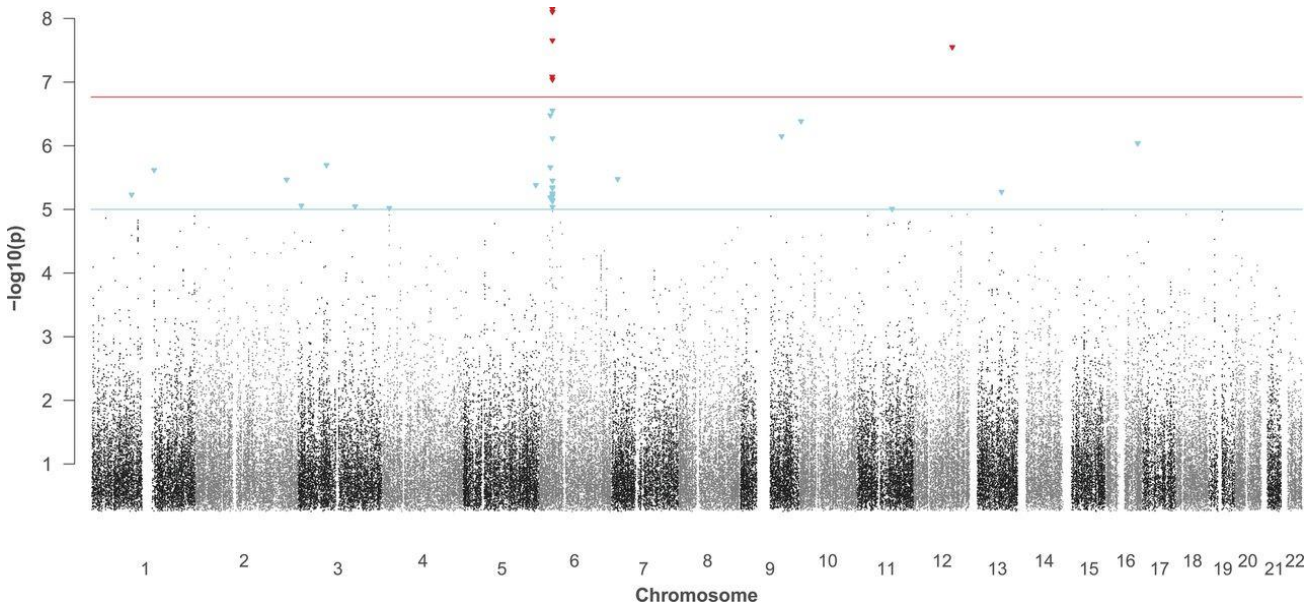

Figure 3.2 : A manhattan plot of the genome-wide association study for dilated cardiomyopathy. Minus log10 *P*-values based on an additive genetic model are shown for single nucleotide polymorphisms that passed the quality control criteria for the screening cohort. Probability values were based on a logistic regression model, which also included age and sex. The red line indicates the genome-wide significance level of $P = 1.7 \times 10^{-7}$ and the blue line indicates the suggestive significance level of $P = 10^{-5}$.

Figure 3.3

miRNA expression levels correlate with disease severity. Matrix plots visualize the correlation of miRNAs from the signature with cardiac systolic function and with NYHA functional class. MiR-622, miR-520d-5p, miR-519e* and miR-200b* significantly correlate with left-ventricular ejection fraction (P < 0.05). No significant correlation could be found between miRNA expression levels and the corresponding NYHA class, although a trend can be observed.	miRNA expression levels correlate with disease severity. Matrix plots visualize the correlation of miRNAs from the signature with cardiac systolic function and with NYHA functional class. MiR-622, miR-520d-5p, miR-519e*, miR-200b*, miR-122* and miR-558 significantly correlate with left-ventricular ejection fraction (P < 0.05). No significant correlation could be found between miRNA expression levels and the corresponding NYHA class, although a trend can be observed.

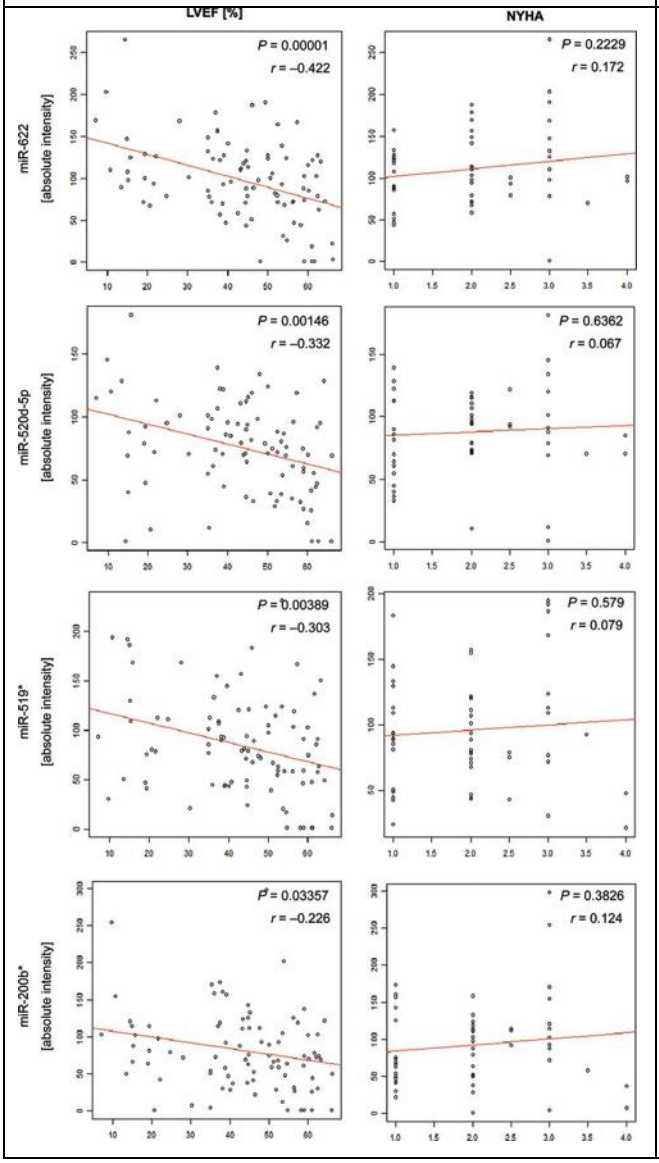

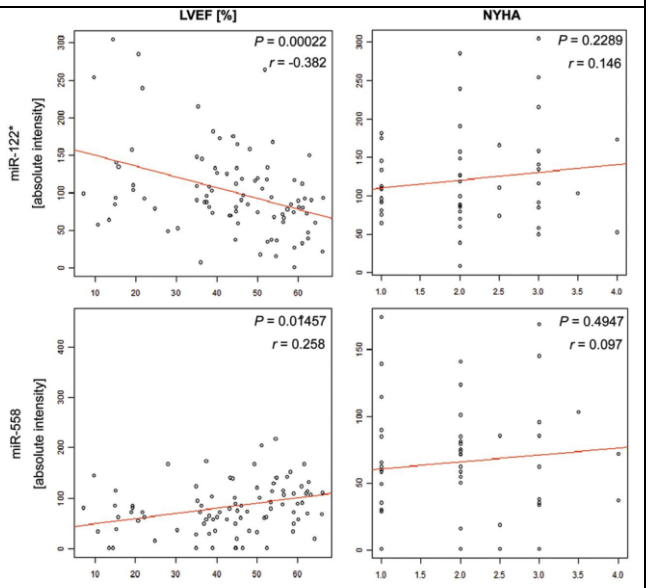

WP4 Transcriptomics

Figure.4.1

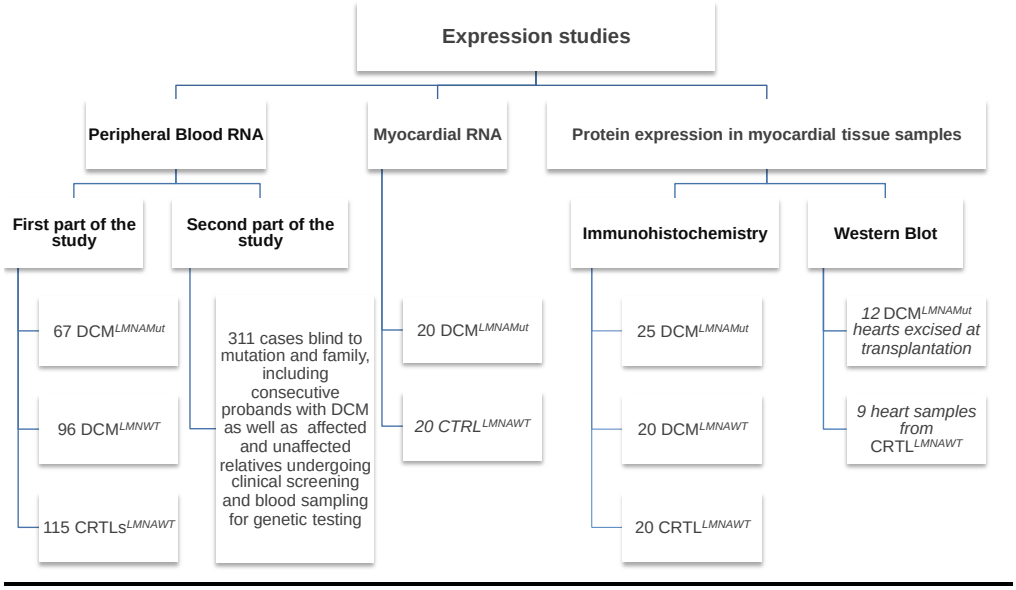

Figure 4.1: The figure summarizes the flow chart of the research for quantitative expression of LMNA in myocardial samples and in peripheral blood samples.

Figure.4.2

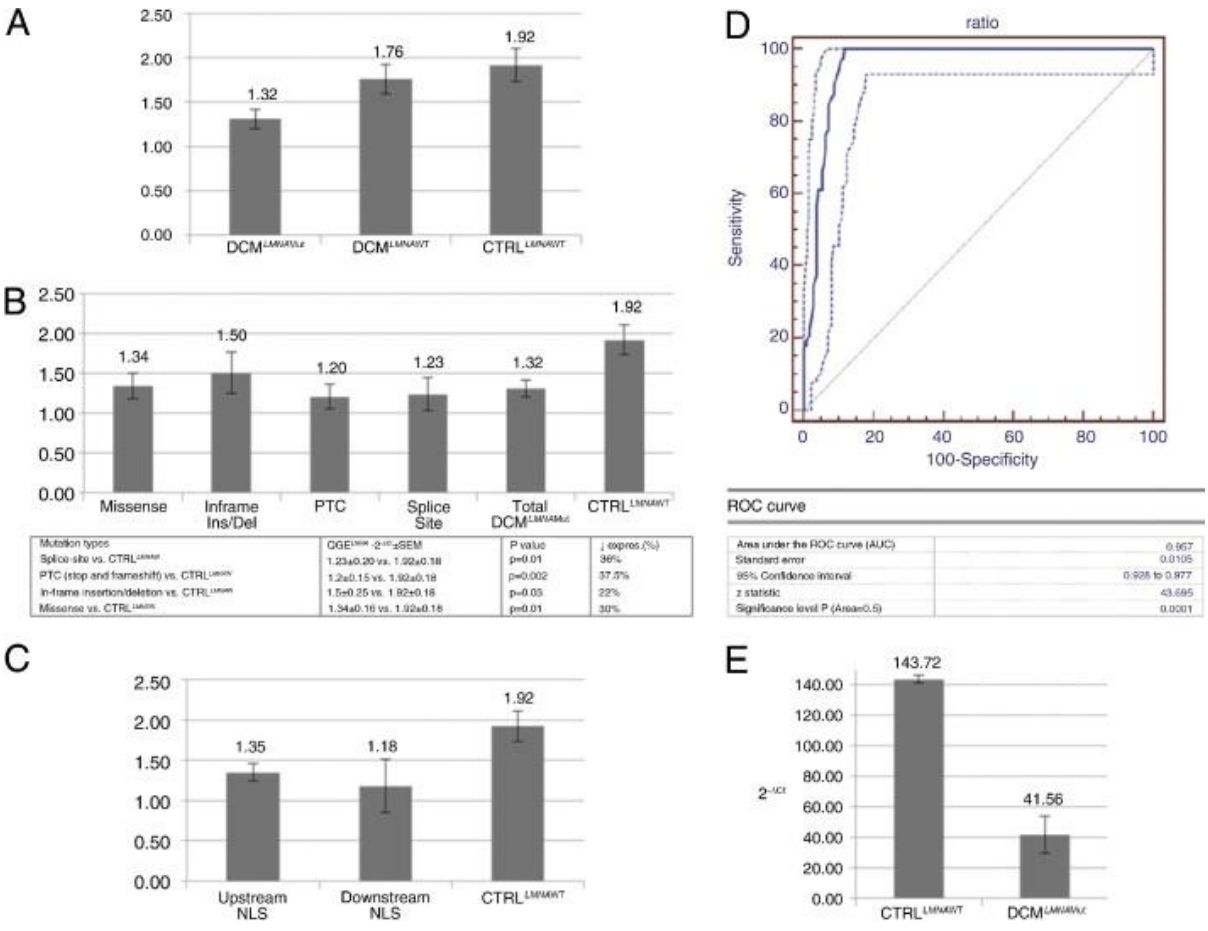

Figure 4.2: QGE*LMNA* Study **(A to C)** First part of the study: QGE*LMNA* ($2^{-\Delta Ct}$ ± SEM) in total RNA from peripheral blood of 67 DCM*LMNA*^{Mut}, 96 DCM*LMNA*^{WT}, and 115 CTRL*LMNA*^{WT}. **(B)** QGE*LMNA* levels did not vary in patients with different types of mutations, and **(C)**with mutations localized upstream or downstream of the nuclear localizing sequence (NLS). **(D)** Second part of the study: receiver-operating characteristic (ROC) curve analysis for the QGE*LMNA* in the peripheral blood RNA from the 311 consecutive cases. At the threshold value with the highest sensitivity, the area under the curve (AUC) was 0.957 ($p < 0.001$). **(E)** Third part of the study: myocardial samples of DCM*LMNA*^{Mut} versus CTRL*LMNA*^{WT}. CTRL = normal control; DCM = dilated cardiolaminopathy; PTC = premature termination codon; QGE = quantitative gene expression.

Figure. 4.3

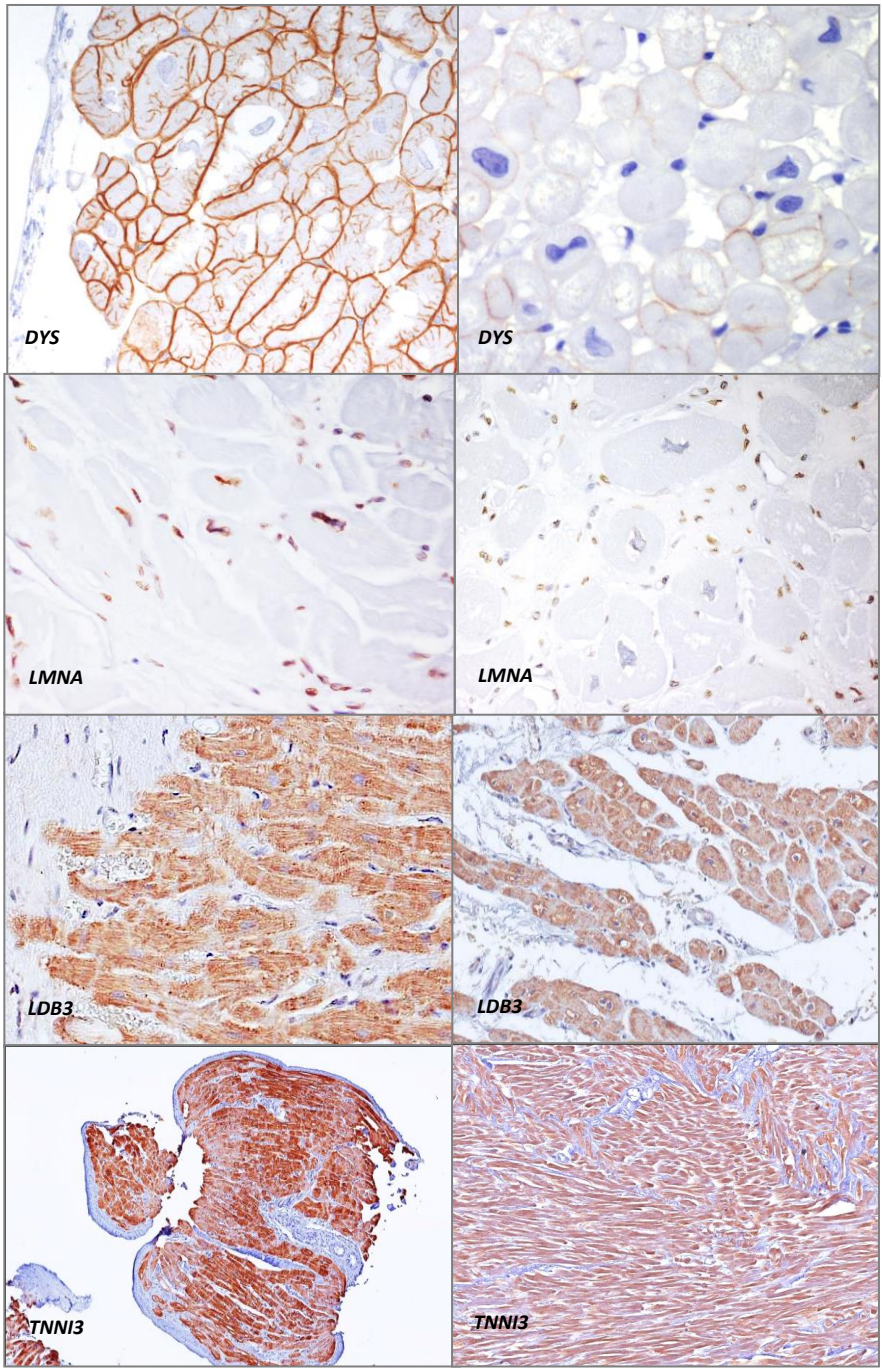

Figure. 4.3 : The panels shows the most striking results in dystrophinopathies in which immunohistochemistry strongly supports the diagnosis (mut vs. WT); in cardiolaminopathies in which immunohistochemisrty can contribute to suspect a mutation in LMNA (mut vs. WT); in cardiozaspopathies (LDB3) and trpoponinopathies in which immunohistochemistry does not discriminate or show significant difference of the expression of the protein in mutated and wild type control samples. The translational impact of these results is therefore relevant for cardiodystrophinopathies and cardiolaminopathies but non-contributory to cardiozaspopathies.

WP5 Proteomics & metabolomics

Figure. 5.1

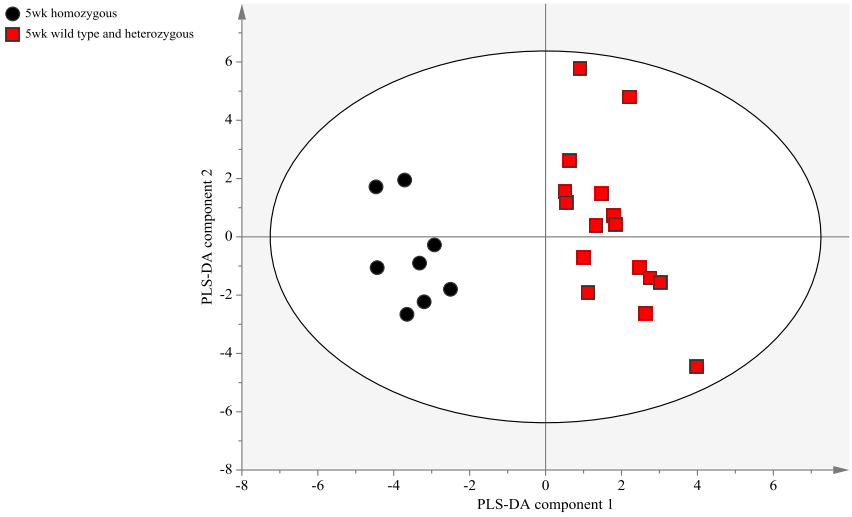

Figure. 5.1: Scores plot comparing aqueous metabolites detected by HILIC mode chromatography from heart tissue from wild type and heterozygous mice (one group) with homozygous laminopathic mouse hearts at the 5-week time point (model parameters R^2X=41%, R^2Y=93%, Q^2=78%).

Figure 5.2

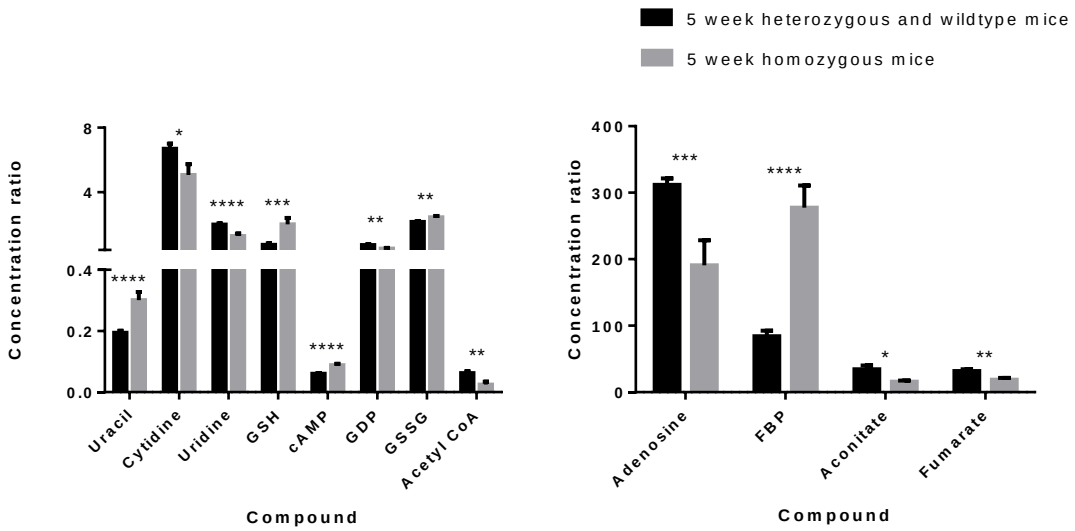

Figure. 5.2: Histograms summarising the significant metabolic changes between the homozygous and the combined group of heterozygous and wild type mice when analysed by HILIC chromatography. Standard error bars are shown and Student's t tests have been carried out (Key: * = $p < 0.05$, ** = $p < 0.01$, *** = $p < 0.001$, **** = $p < 0.0001$).

WP6 Animal models: zebra fish

Figure. 6.1

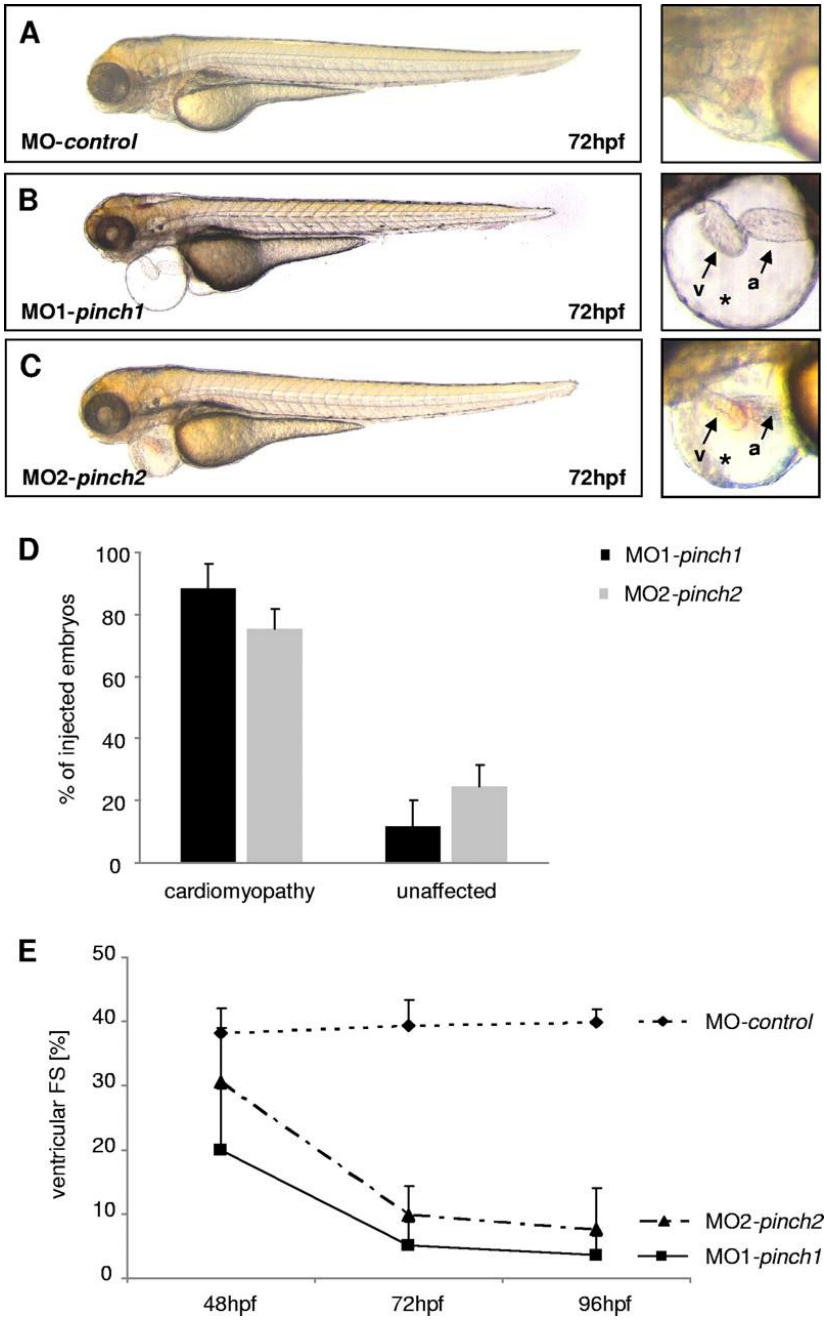

Figure.6.1: Knockdown of PINCH1 or PINCH2 leads to cardiomyopathy and heart failure. (A to C) MO1-*pinch1*- and MO2-*pinch2*-injected embryos develop pericardial oedema (*) and pericardial blood congestion due to disturbed cardiac contractility. Lateral Views of MO-*control*-injected (A), MO1-*pinch1*-injected (B)

and MO2-*pinch2*-injected (C) embryos at 72 hours hpf (v, ventricle; a, atrium). (D) After injection of MO1-*pinch1* or MO2-*pinch2*, 88% and 75% of morphant embryos, respectively, develop heart failure. (E) FS of the ventricular chambers of MO-*control*-, MO1-*pinch1*-, and MO2-*pinch2*-injected embryos measured at the indicated developmental stages. FS is significantly reduced in PINCH mophants after 48 hpf and further declines by 96 hpf.

Figure 6.2

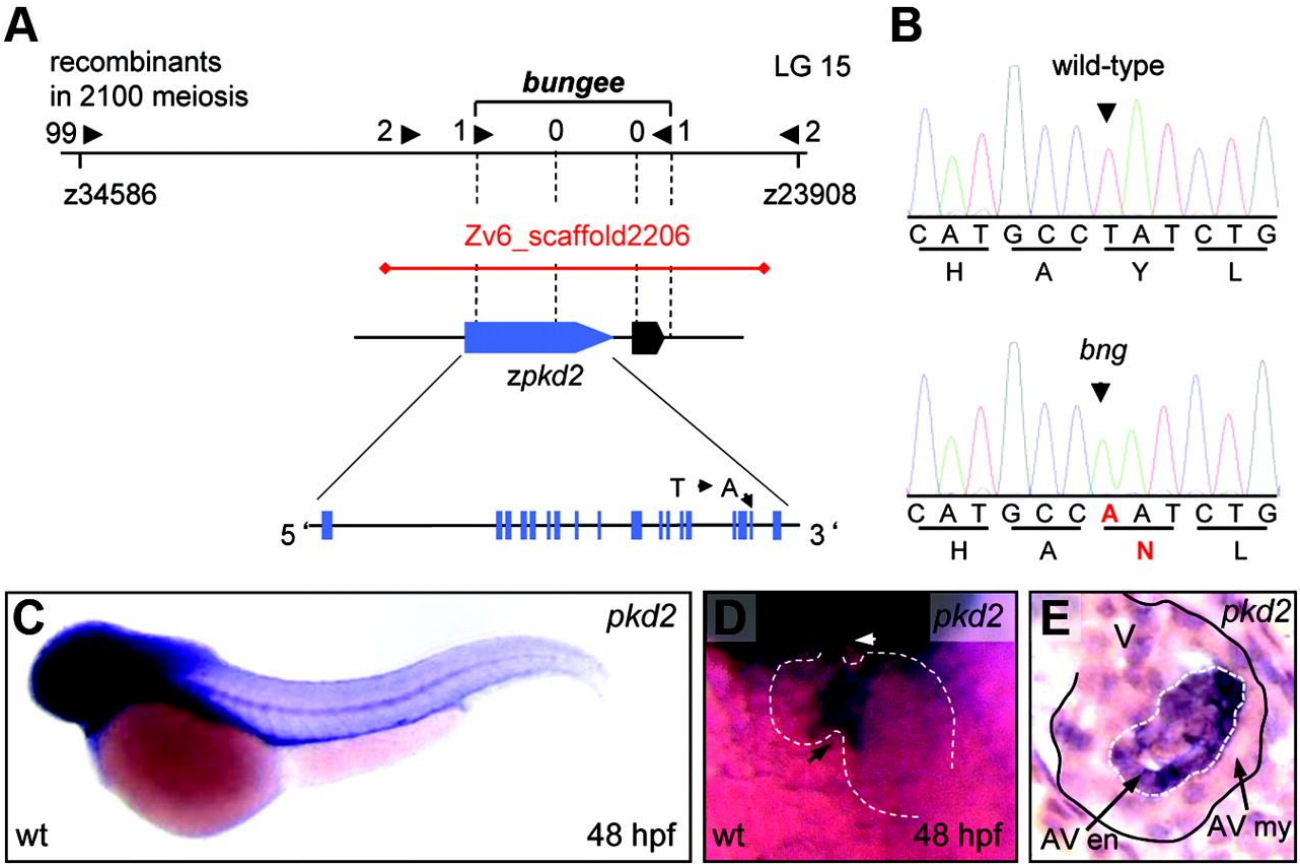

Figure 6.2 :bng encodes protein kinase D2 (pkd2) and is expressed in the zebrafish atrioventricular canal (AVC). A, Integrated genetic and physical map of the bng locus on zebrafish chromosome 15.
The bng mutation interval is flanked by the microsatellite markers z34586 and z23908 and encodes 2 open reading frames, zebrafish pkd2 and an unknown protein (zgc:152692). The genomic structure of zebrafish pkd2 (zpkd2) is displayed at the bottom. The bng missense mutation (T→A) in the 17th exon of zpkd2 is indicated. B, The bng missense mutation at cDNA position 2545 translates into an amino acid exchange from tyrosine (T) to asparagine (N). An arrowhead marks the mutated base. C through E, Whole-mount antisense RNA in situ hybridization of zebrafish pkd2 expression in the brain, gastrointestinal tract, and AVC (black arrow) of the heart of zebrafish embryos at 48 hours after fertilization (hpf; C and D). E, Detection of pkd2 in atrioventricular endocardial (AV en) but not AV myocardial (AV my) cells at 72 hpf by whole-mount antisense RNA in situ hybridization of a sagittal section through the atrioventricular canal of a zebrafish heart.

WP7 Animal models: LMNA KO mice

Figure 7.1 LMNA

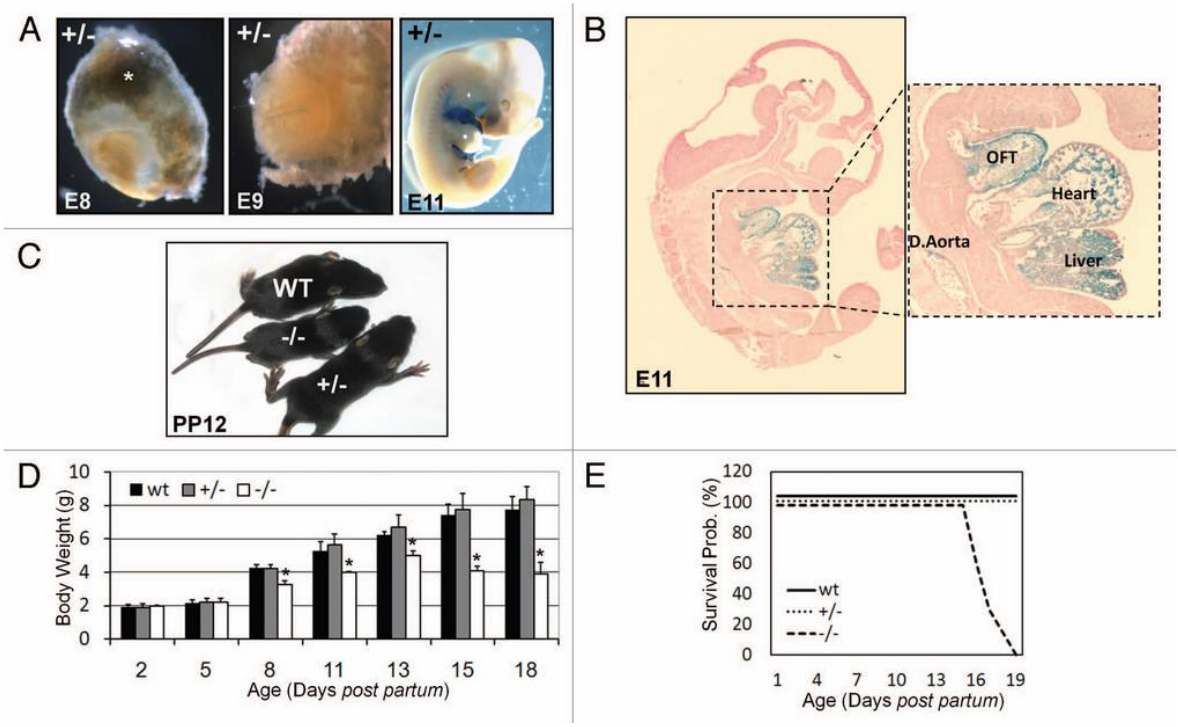

Figure. 7.1: Embryonic and postnatal phenotypical characterization of the *LMNA*GT−/−mouse.

(A) *LMNA* promoter activity is visualized by β-galactosidase staining in *LMNA*GT+/− embryo's (E8.0, E9.0, E11.0). *LMNA*GT+/− placental tissue is indicated by an asterisk.

(B) β-galactosidase stained *LMNA*GT+/−embryo E11.0 tissue section (7 µm) counterstained with Azo Phloxine (magnification 2.5×), including a close-up image (magnification 5.0×) of the heart, the heart's outflow tract (OFT), liver and dorsal aorta (D. Aorta).

(C) Macroscopical view of WT, *LMNA*GT+/−and *LMNA*GT−/− siblings 12 days post partum (PP12).

(D) Body weight over time graph (PP2–PP18). Asterisks indicate a significant difference for *LMNA*GT−/− to *LMNA*GT+/− and WT littermates (N = 10, $p < 0.05$).

(E) Survival curves for all three genotypes (N = 10) during the first 3 weeks post partum.

WP8 Structural studies

Figure. 8.1

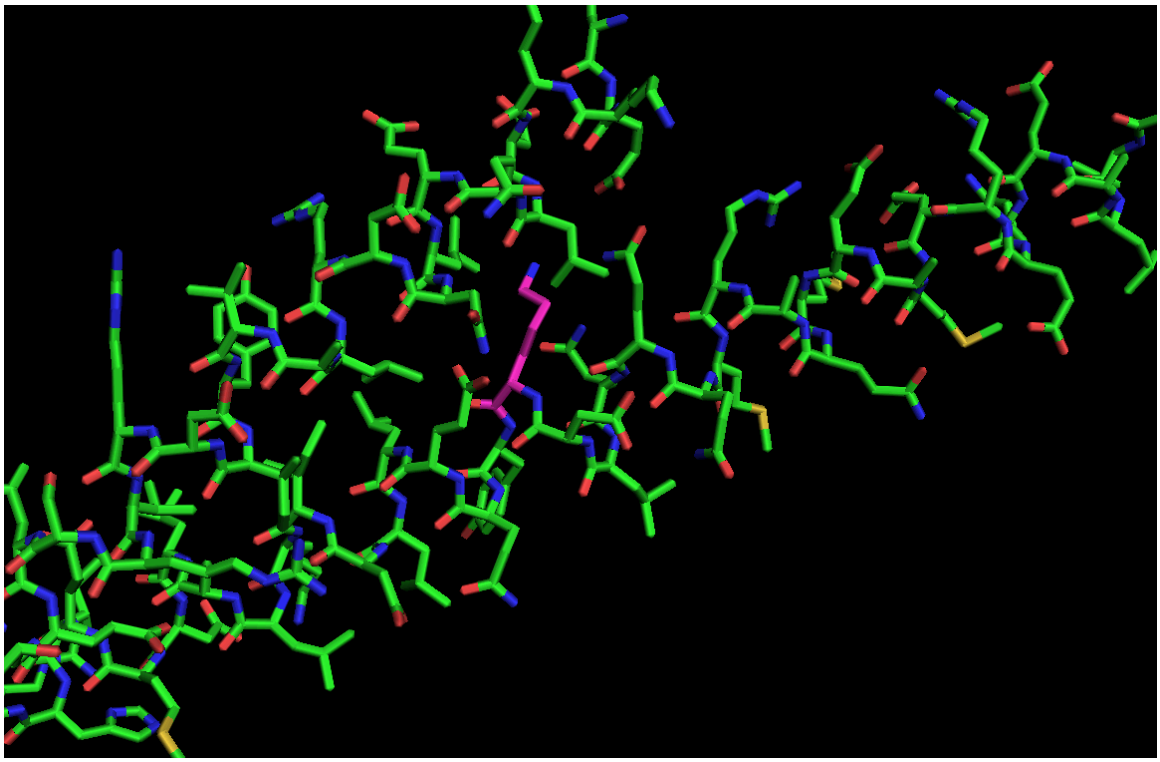

Figure. 8.1: Docking model of the E358K mutant (the mutated residue is represented in purple)

Figure. 8.2

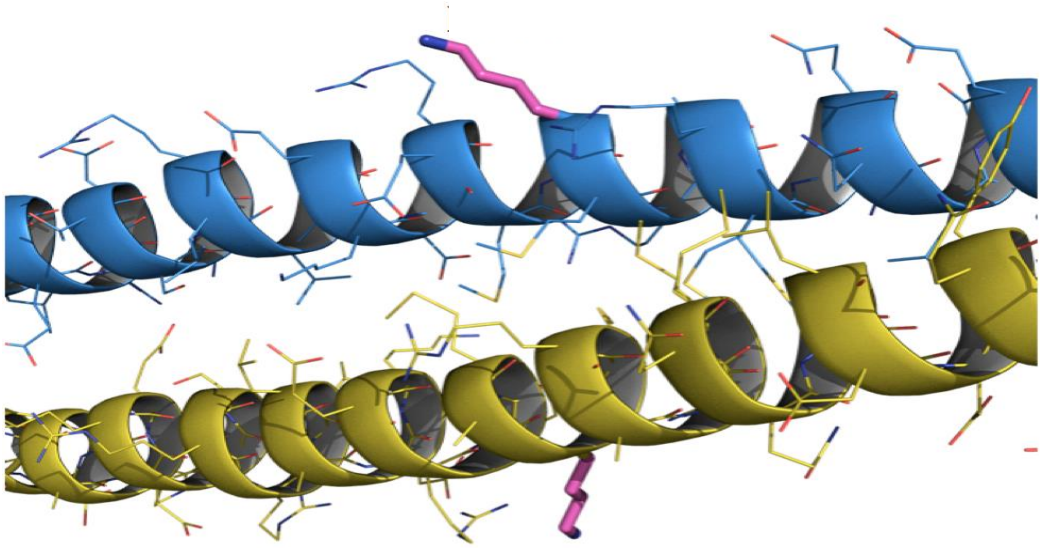

Figure.8.2: Crystal structures of E347K. View of the mutated region. Substituted residue is in red.

WP9 Therapeutics and improvement of medical management

Figure.9.1

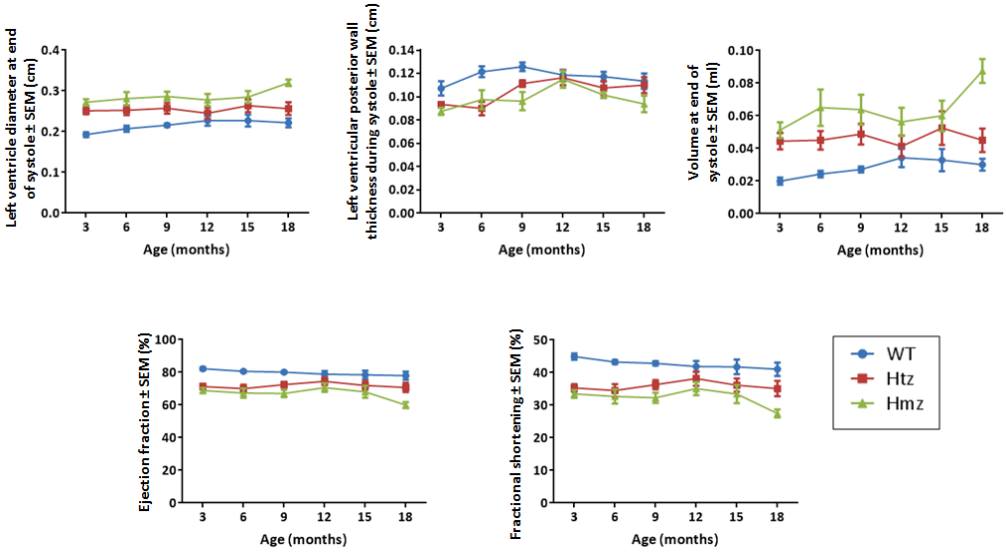

Figure 9.1: Graphs of described echocardiographic measures over nine months in male Mypn KI mice of the three genotypes. Homozygous measures were generally significantly different to wild-type at all time points across each of the variables shown, using 2-way ANOVA ($p < 0.05$ to 0.001), and heterozygous values were often significantly different to wild-type values.
Over time, values for all three genotypes did not differ significantly – except for posterior wall systolic thickness in heterozygous mice – indicating that a cardiac phenotype may not be appreciably worsening. All parameters shown were generally not significantly different between heterozygote and homozygote animals. WT = wild-type, Htz = heterozygote, Hmz = homozygote. Error bars are SEM, n = 7 to 8 animals per group.

Figure. 9.2

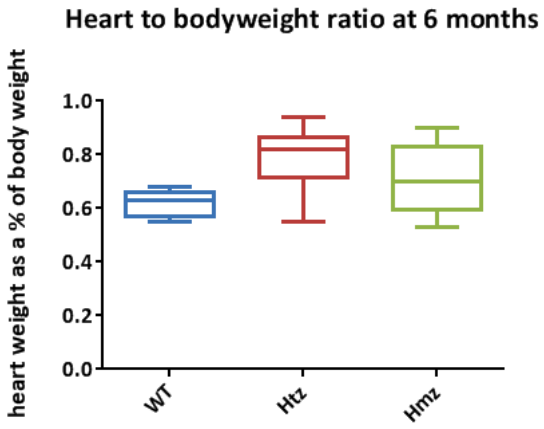

Figure 9.2: Heart to body weight ratio at six months. Homozygous and heterozygous mouse hearts are respectively ~11 to 30% larger at the age of six months compared to wild-type mice; $p < 0.05$

only for WT vs. Htz mice, Student's unpaired t-test. WT = wild-type, Htz = heterozygotes, Hmz = homozygotes. n = 7 to 8 mice for each group.

Figure. 9.3

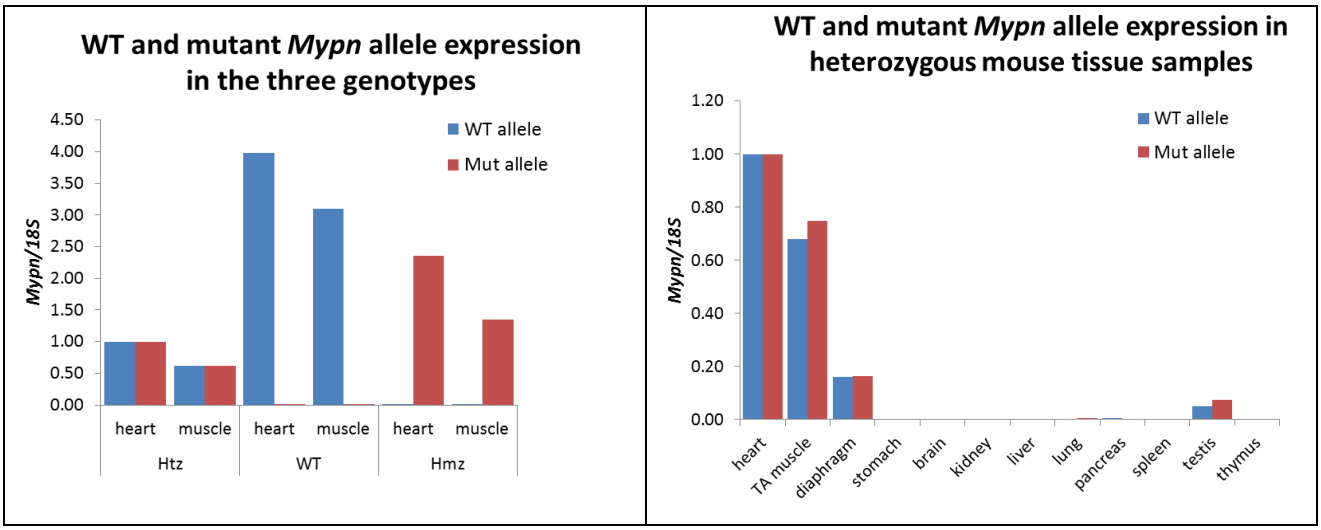

Figure 9.3: Allele-specific qPCR results indicating that A. The qPCR is specific, and that equal amounts of WT and mutant alleles are expressed in the heterozygous mouse, and that
B. Myopalladin expression is limited to skeletal and cardiac muscles, excepting very low expression in the testes.

Figure.9.4

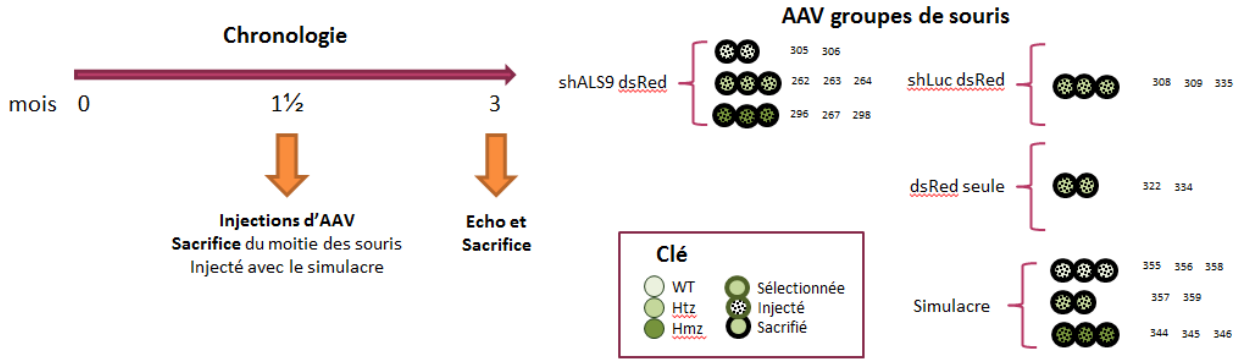

Figure 9.4: Experimental outline for testing AAV2.9 viruses.
Six-week-old Mypn KI mice will be infected with AAV2.9-shALS9-dsRed, AAV2.9-shLuc-dsRed, AAV2.9-dsRed or a mock injection via the retro-orbital route.
Six weeks post-injection, the mice with undergo echographic analysis, and will then be sacrificed for molecular analysis.

WP 10 Bioinformatics Database

Figure 10.1

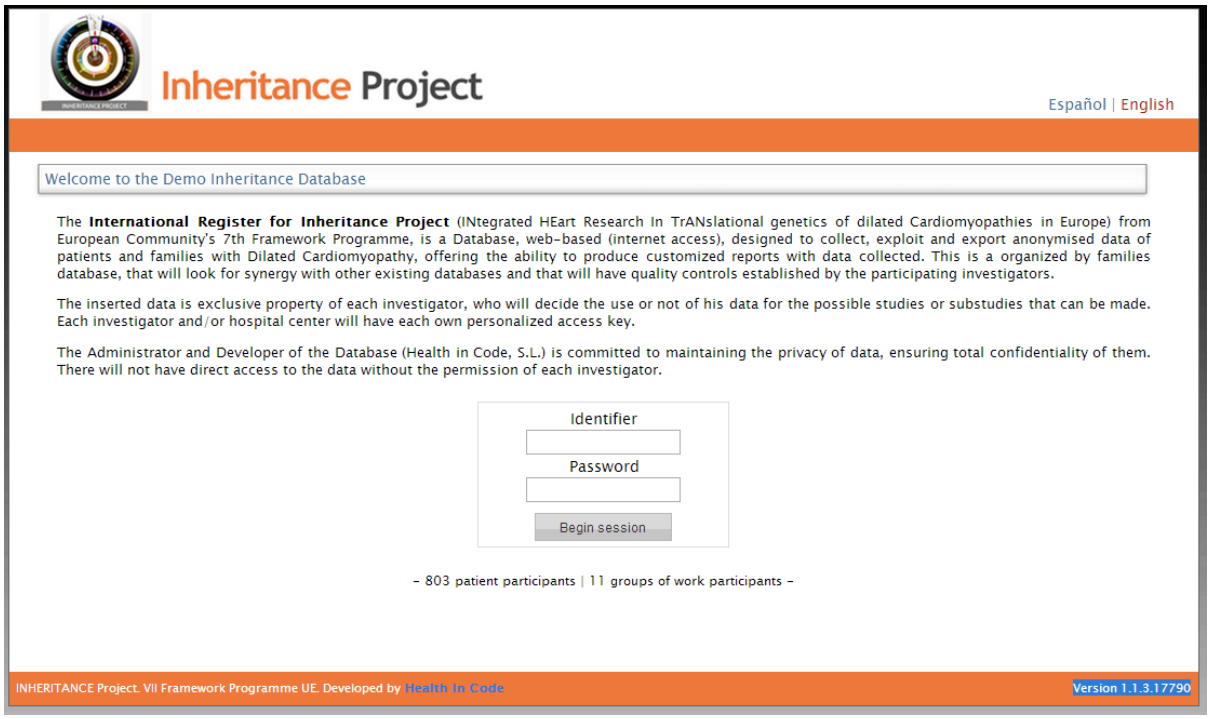

Figure 10.2

WP 11 Knowledge management Bioinformatics Database and data analysis

Figure. 11.1

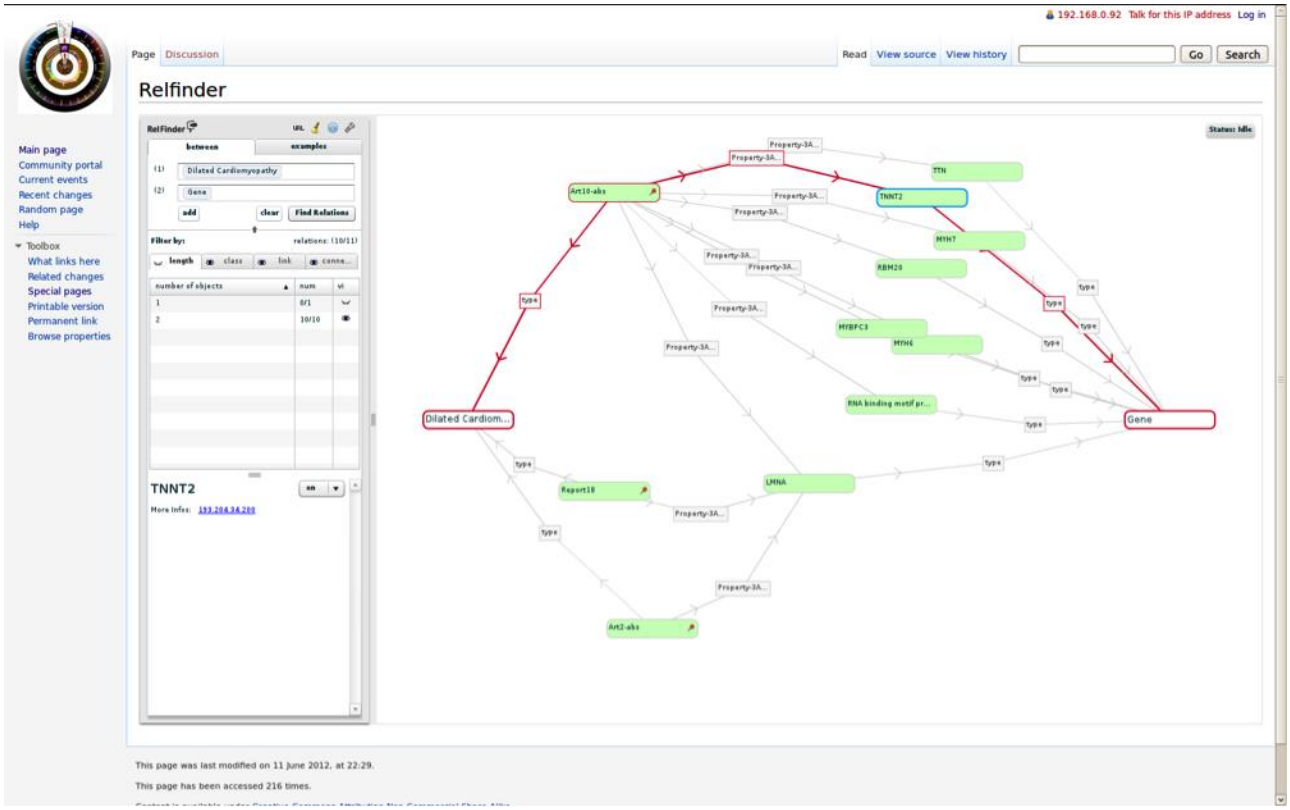

Figure 11.2

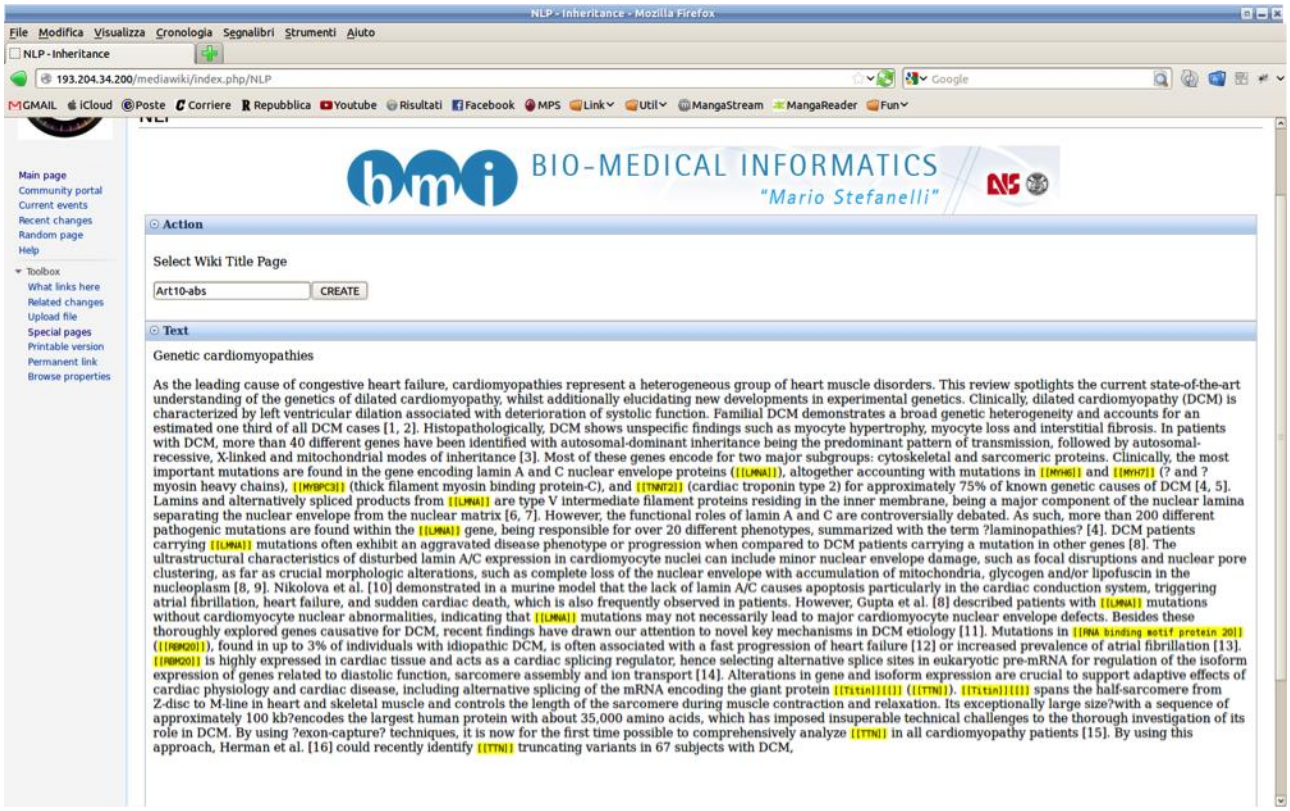

Potential Impact

Potential Impact Figure 1.

The figure summarizes the key issues in INHERITANCE: at the centre, a dilated heart excised at transplantation; the logo on its left is a miniature of a family tree, DNA, disease genes, cells. Around the heart and logo, family trees before and after family screening and follow-up. The pair of upper pedigrees correspond to a LMNA family before and after genetic testing; the lower pedigrees correspond to a DYS family before and after genetic testing and follow-up; electropherograms as in Sanger sequencing; loss of protein expression in mutated hearts (Lamin AC , western blot of wild type and mutated Lamin AC on the right; immunohistochemistry: Lamin AC on the left; dystrophin on the right.

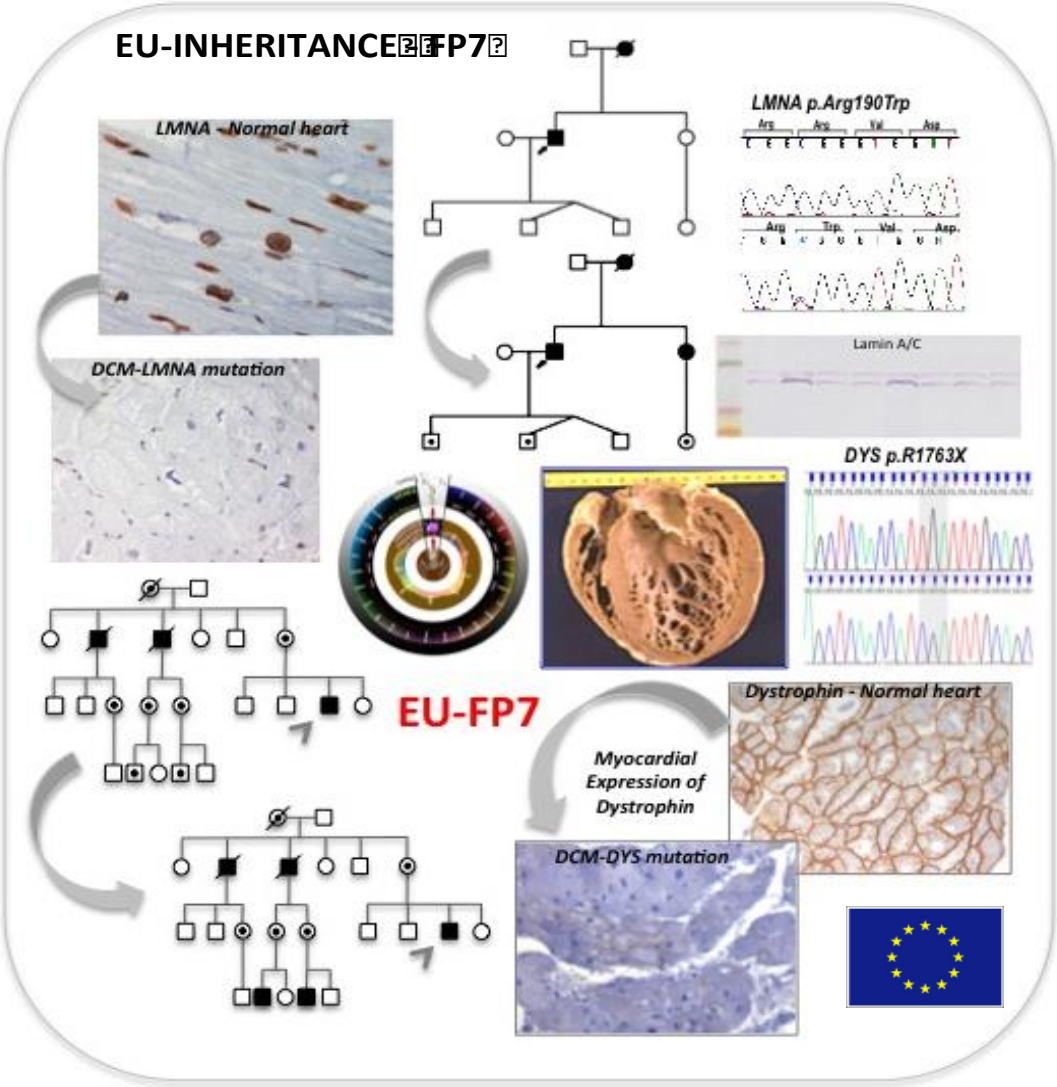

Potential Impact Figure 2.

A) The discipline-centred model of care obligates patients and families to search multispecialty support

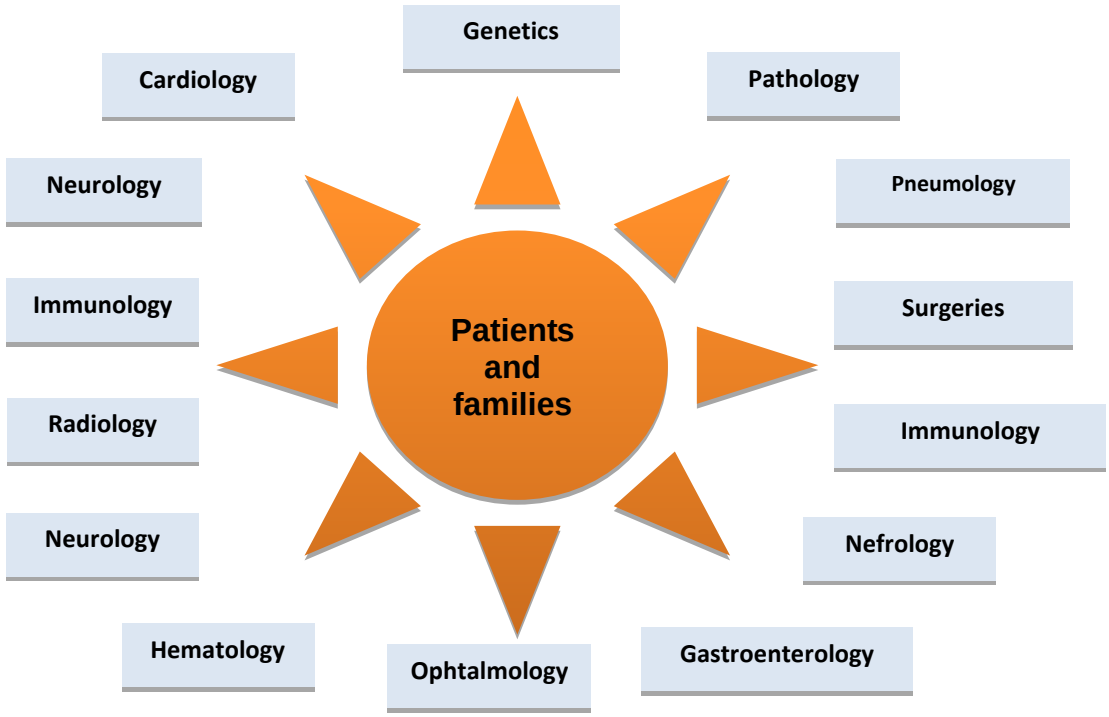

B) The patient/family-centred model of care places the patient and his/her family at the middle core of the diagnostic work-up, plans specialist interventions on the individual needs and care plans.

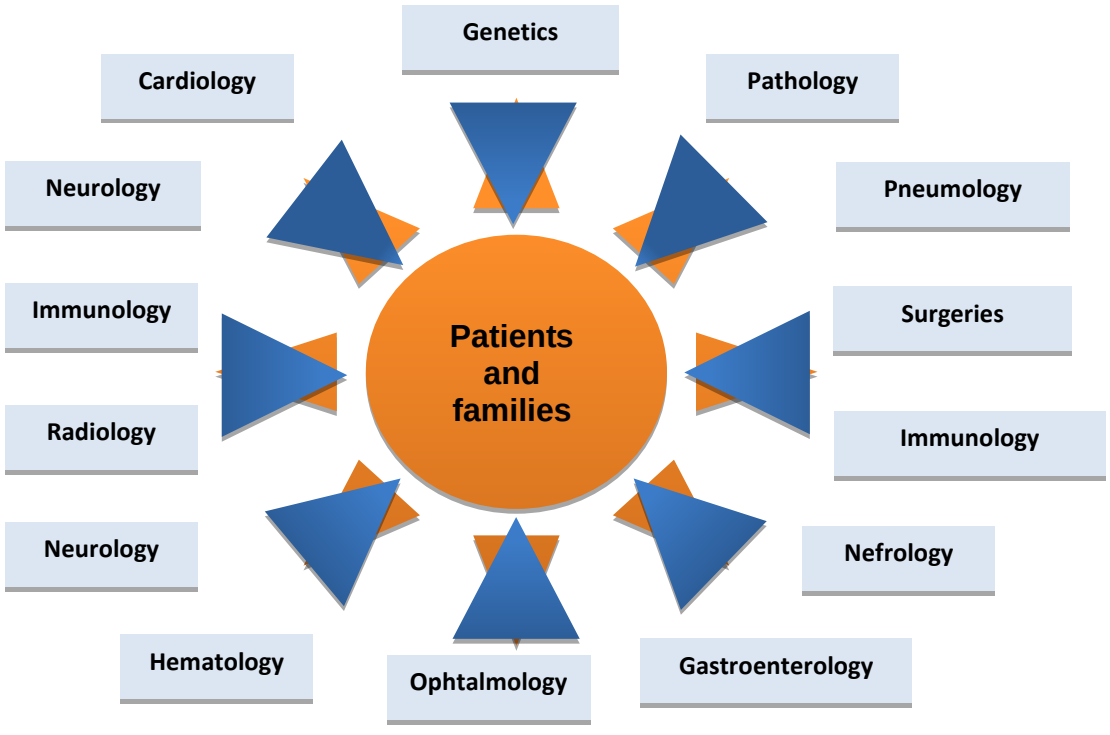

Potential impact Figure 3

In a few weeks after publication, MOGE (S) attracted the attention of the scientific international community and opened the discussion about the need of a novel nosology system that describes both phenotype and genotype (Panel from the web sites).

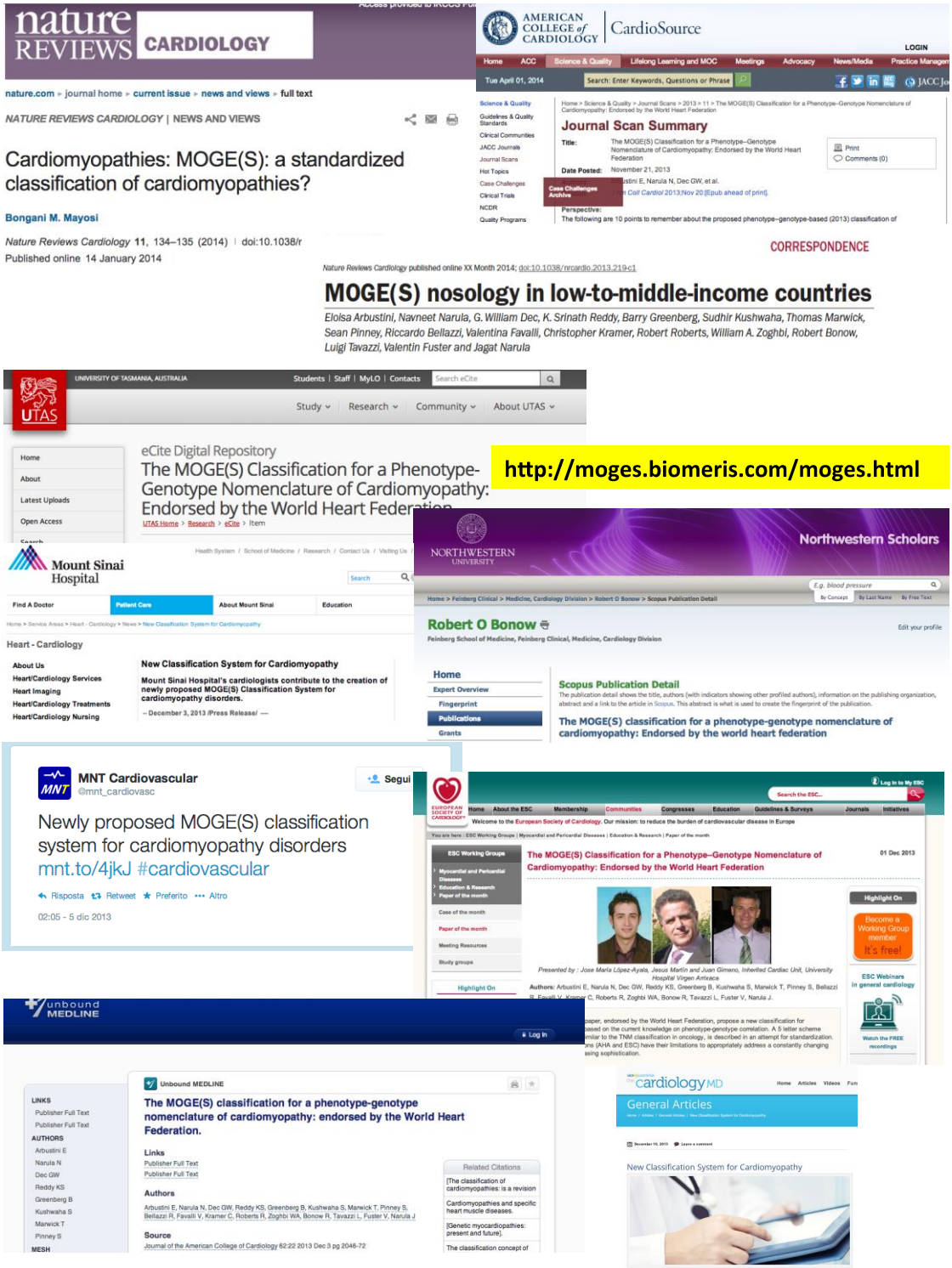

List of beneficiaries and contacts

Beneficiary Number	Beneficiary name	Beneficiary short name	Country
1 Coordinator	**Academic Hospital IRCCS Foundation Policlinico San Matteo (OSM) – Centre for Inherited Cardiovascular Diseases -** P. Golgi 19, 27100 Pavia, Italy. Phone: +39-0382-501486; fax: +39-0382-501893; e-mail: info.cardiomiopatie@smatteo.pv.it	OSM	IT
2	**The Heart Hospital, University College London NHS Foundation Trust** – The Heart Hospital, 16-18 Westmoreland Street, London W1G 8PH, United Kingdom. Phone: +44-20-7573 8888; fax: +44-20-7573 8838.	UCL	UK
3	**Heart Centre, Department of Medicine - Umeå University Hospital - S-901 85 Umeå, Sweden**	UUH	SW
4	**Universitätsklinikum Heidelberg, Im Neuenheimer Feld 410, 69120 Heidelberg, Germany.** Phone: +49-6221-56-8670; fax: +49-6221-56-5516.	UKLHD	DE
5	**Institut National De La Sante et De La Recherche Medicale (INSERM)** – 101 Rue de Tolbiac 75654 Paris, France - Phone: +33-142162898; fax: +33142161364.	INSERM	FR
6	**Health in Code SL (SME) -** Hospital Marítimo de Oza. Edificio Fortín. As Xubias SN. A Coruña 15006. Spain. Phone:+34981167000 ext 5929; fax: +34981138714; e-mail: info@healthincode.com	HIC	ES
7	**The Department of Biochemistry, University of Cambridge -** Tennis Court Road, Cambridge, CB2 1GA UK Phone: +44-1223 333667; fax +44-1223 766002	UCAM	UK
8	**Centre for Hereditary Cardiac Conditions,** Department of Cardiology, Skejby Hospital, Aarhus University Hospital, Brendstrupgaardsvej, 8200 Aarhus N, Denmark. Phone: +45 89496199; fax: +45 89496002	SUH	DK
9	**Academic Medical Center and InterUniversity Institute Netherlands,** The Heart Failure Research - AMC/ICIN. Phone: 31-20-5664927	AMC	NDL
10	**Università degli Studi di Pavia, Department of Computer Engineering and Systems Science -** Via Ferrata 1, 27100 Pavia Phone:+39-0382-985720; fax: +39-0382-525638	UNIPV	IT
11	**Department of Biomolecular Sciences and Biotechnology**, University of Milano, Via Celoria 26, Milano, Italy. Phone: +39 02-50314893; fax: +39-0250314895	UMIL	IT

SCIENTIFIC PRODUCTS

N.	Papers	IF – SCI 2012
1	Jan Haas, Karen S. Frese, Barbara Peil, Wanda Kloos, Andreas Keller, Rouven Nietsch, Zhu Feng, Sabine Müller, Elham Kayvanpour, Britta Vogel, Farbod Sedaghat-Hamedani, Wei-Keat Lim, Xiaohong Zhao, Dmitriy Fradkin, Doreen Köhler, Simon Fischer, Jennifer Franke, Sabine Marquart,Ioana Barb, Ali Amr, Philipp Ehlermann, Derliz Mereles, Tanja Weis, Andreas Kremer, Vanessa King, Emil Wirsz, Richard Isnard, Michel Komajda, Alessandra Serio, Maurizia Grasso, Petros Syrris, Eleanor Wicks, Vincent Plagnol, Luis Lopes, Tenna Gadgaard, Hans Eiskjær, Mads Jørgensen, Diego Garcia-Giustiniani, Martin Ortiz-Genga, Maria G. Crespo-Leiro, Rondal H. Lekanne Dit Deprez, Imke Christiaans, Ingrid A. van Rijsingen, Arthur A. Wilde, Anders Waldenstrom, Martino Bolognesi, Riccardo Bellazzi, Stellan Mörner, Justo Lorenzo Bermejo, Lorenzo Monserrat, Eric Villard, Jens Mogensen, Yigal M. Pinto, Philippe Charron, Perry Elliott, Eloisa Arbustini, Hugo A. Katus, Benjamin Meder. Atlas of the Clinical Genetics of Human Dilated Cardiomyopathy Eur Heart J (under evaluation) 2014.	14.086
2	de Haas HJ, Arbustini E, Fuster V, Kramer CM, Narula J. Molecular imaging of the cardiac extracellular matrix. Circ Res. 2014;114:903-15.	11.861
3	Arbustini E, Narula N, Dec GW, Reddy KS, Greenberg B, Kushwaha S, Marwick T, Pinney S, Bellazzi R, Favalli V, Kramer C, Roberts R, Zoghbi WA, Bonow R, Tavazzi L, Fuster V, Narula J. MOGE(S) nosology in low-to-middle-income countries. Nat Rev Cardiol. 2014 Mar 25. doi: 10.1038/nrcardio.2013.219-c1.	10.400
4	Arbustini E, Narula N, Dec GW, Reddy KS, Greenberg B, Kushwaha S, Marwick T, Pinney S, Bellazzi R, Favalli V, Kramer C, Roberts R, Zoghbi WA, Bonow R, Tavazzi L, Fuster V, Narula J. Response Letter to J Am Coll Cardiol. 2014	14.086
5	Narula N, Agozzino M, Gazzoli F, Concardi M, Pagani F, Favalli V, Kodama T, Mazzola A, D'Armini AM, Arbustini E. The pathologic basis of recovery. Heart Fail Clin. 2014;10:S63-74.	2.5
6	Arbustini E, Narula N, Dec GW, Reddy KS, Greenberg B, Kushwaha S, Marwick T, Pinney S, Bellazzi R, Favalli V, Kramer C, Roberts R, Zoghbi WA, Bonow R, Tavazzi L, Fuster V, Narula J. The MOGE(S) Classification for a Phenotype-Genotype Nomenclature of Cardiomyopathy: Endorsed by the World Heart Federation. J Am Coll Cardiol. 2013;62:2046-72.	14.086
7	Arbustini E, Narula N, Dec GW, Reddy KS, Greenberg B, Kushwaha S, Marwick T, Pinney S, Bellazzi R, Favalli V, Kramer C, Roberts R, Zoghbi WA, Bonow R, Tavazzi L, Fuster V, Narula J. The MOGE(S) Classification for a Phenotype-Genotype Nomenclature of Cardiomyopathy: Endorsed by the World Heart Federation. G Heart. 2013; 8:355-382.	
8	Vogel B, Keller A, Frese KS, Leidinger P, Sedaghat-Hamedani F, Kayvanpour E, Kloos W, Backe C, Thanaraj A, Brefort T, Beier M, Hardt S, Meese E, Katus HA, Meder B. Multivariate miRNA signatures as biomarkers for non-ischaemic systolic heart failure. Eur Heart J. 2013;34:2812-22.	14.097
9	Disertori M, Quintarelli S, Mazzola S, Favalli V, Narula N, Arbustini E. The need to modify patient selection to improve the benefits of implantable cardioverter-defibrillator for primary prevention of sudden death in non-	2.765

	ischaemic dilated cardiomyopathy. Europace. 2013;15:1693-701.	
10	Rasmussen TB, Hansen J, Nissen PH, Palmfeldt J, Dalager S, Jensen UB, Kim WY, Heickendorff L, Mølgaard H, Jensen HK, Sørensen KE, Baandrup UT, Bross P, Mogensen J. Protein expression studies of desmoplakin mutations in cardiomyopathy patients reveal different molecular disease mechanisms. Clin Genet. 2013;84:20-30.	4.247
11	Rasmussen TB, Palmfeldt J, Nissen PH, Magnoni R, Dalager S, Jensen UB, Kim WY, Heickendorff L, Mølgaard H, Jensen HK, Baandrup UT, Bross P,Mogensen J. Mutated desmoglein-2 proteins are incorporated into desmosomes and exhibit dominant-negative effects in arrhythmogenic right ventricular cardiomyopathy. Hum Mutat, 2013;34:697-705	5.213
12	Heather LC, Wang X, West JA, Griffin JL. A practical guide to metabolomic profiling as a discovery tool for human heart disease. J Mol Cell Cardiol. 2013;55:2-11.	5.148
13	Meder B, Rühle F, Weis T, Homuth G, Keller A, Franke J, Peil B, Lorenzo Bermejo J, Frese K, Huge A, Witten A, Vogel B, Haas J, Völker U, Ernst F, Teumer A, Ehlermann P, Zugck C, Friedrichs F, Kroemer H, Dörr M, Hoffmann W, Maisch B, Pankuweit S, Ruppert V, Scheffold T, Kühl U, Schultheiss HP, Kreutz R, Ertl G, Angermann C, Charron P, Villard E, Gary F, Isnard R, Komajda M, Lutz M, Meitinger T, Sinner MF, Wichmann HE, Krawczak M, Ivandic B, Weichenhan D, Gelbrich G, El-Mokhtari NE, Schreiber S, Felix SB, Hasenfuß G, Pfeufer A, Hübner N, Kääb S, Arbustini E, Rottbauer W, Frey N, Stoll M, Katus HA. A genome-wide association study identifies 6p21 as novel risk locus for dilated cardiomyopathy. Eur Heart J. 2013 Jul 12. [Epub ahead of print]	14.097
14	Haas J, Frese KS, Park YJ, Keller A, Vogel B, Lindroth AM, Weichenhan D, Franke J, Fischer S, Bauer A, Marquart S, Sedaghat-Hamedani F, Kayvanpour E, Köhler D, Wolf NM, Hassel S, Nietsch R, Wieland T, Ehlermann P, Schultz JH, Dösch A, Mereles D, Hardt S, Backs J, Hoheisel JD, Plass C, Katus HA, Meder B. Alterations in cardiac DNA methylation in human dilated cardiomyopathy. EMBO Mol Med. 2013;5:413-29.	7.759
15	Frese KS, Katus HA, Meder B. Next-Generation Sequencing: From Understanding Biology to Personalized Medicine. Biology 2013, 2, 378-398	
16	Larizza C, Gabetta M, Milani G, Bucalo M, Mulas F, Nuzzo A, Favalli V, Arbustini E, Bellazzi R. Supporting translational research on inherited cardiomyopathies through information technology. Methods Inf Med. 2013;52:137-47.	1.6
17	van Rijsingen IAW, Nannenberg EA, Arbustini E, Elliott PM, Mogensen J, Hermans-van Ast JF, van der Kooi AJ, van Tintelen JP, van den Berg MP, Grasso M, Serio A, Jenkins S, Rowland C, Richard P, Wilde AAM, Perrot A, Pankuweit S, Zwinderman AH, Charron P, Christiaans I, Pinto YM. Gender-specific differences in major cardiac events and mortality in lamin A/C mutation carriers. *Eur J Heart Fail*. 2013;15:376-84	5.247
18	Thanaraj A, Meder B. Genetic testing is superior to biopsy of the myocardium in cardiomyopathy - yes. Dtsch Med Wochenschr. 2013;138:598	0.65
19	Kodama T, Serio A, Disertori M, Bronzetti G, Diegoli M, Narula N, Grasso M, Mazzola S; Arbustini E. Autosomal recessive paediatric sick sinus syndrome associated with novel compound mutations in *SCN5A. Int J Cardiol*. 2013;167:3078-80	5.509

20	Gabetta M, Larizza C, Bellazzi R. A Unified Medical Language System (UMLS) based system for Literature-Based Discovery in medicine. Stud Health Technol Inform. 2013;192:412-6.	
21	Disertori M, Quintarelli S, Grasso M, Pilotto A, Narula N, Favalli V, Canclini C, Diegoli M, Mazzola S, Marini M, Del Greco M, Bonmassari R, Masè M, Ravelli F, Specchia C, Arbustini E. Autosomal recessive atrial dilated cardiomyopathy with standstill evolution associated with mutation of Natriuretic Peptide Precursor A. *Circulation Genetics* 2013 ;6 :27-36.	6.728
22	Kloos W, Katus HA, Meder B. Genetic cardiomyopathies. Lessons learned from humans, mice, and zebrafish. *Herz.* 2012;37:612-7.	0.779
23	Meder B, Katus HA. Clinical and genetic aspects of hypertrophic and dilated cardiomyopathy. *Internist*. 2012;53:408-14, 417-8.	0.3
24	Serio A, Narula N, Kodama T, Favalli V, Arbustini E. Familial DCM: a clinically and genetically heterogeneous disease? *Herz*. 2012;37:822-829.	0.779
25	van Rijsingen IA, Arbustini E, Elliott P, Mogensen J, Hermans-van Ast JF , Van der Kooi AJ , van Tintelen P, van den Berg M, Pilotto A, Pasotti M, Jenkins S , Rowland C, Aslam U , Wilde A, Perrot A, Pankuweit S, Zwinderman AH, Charron P, Pinto YM. Risk Factors for Malignant Ventricular Arrhythmias in Lamin A/C Mutation Carriers: a European Cohort Study. *JACC* 2012;59:493-500	14.086
26	Narula N, Favalli V, Tarantino P, Grasso M, Pilotto A, Bellazzi R, Serio A, Gambarin FI, Charron P, Meder B, Pinto Y, Elliott PM, Mogensen J, Bolognesi M, Bollati M, Arbustini E. Quantitative expression of the mutated lamin a/c gene in patients with cardiolaminopathy. *J Am Coll Cardiol*. 2012;60:1916-20.	14.086
27	Bollati M, Barbiroli A, Favalli V, Arbustini E, Charron P, Bolognesi M. Structures of the lamin A/C R335W and E347K mutants: Implications for dilated cardiolaminopathies. *Biochem Biophys Res Commun.* 2012;418:217-21	2.484
28	Quarta G, Syrris P, Ashworth M, Jenkins S, Zuborne Alapi K, Morgan J, Muir A, Pantazis A, McKenna WJ, Elliott PM. Mutations in the Lamin A/C gene mimic arrhythmogenic right ventricular cardiomyopathy. *Eur Heart J*. 2012;33:1128-36.	14.097
29	Serio A, Narula N, Frontera A, Isabella Gambarin F, Arbustini E. Prevalence of J-point elevation in families with sudden arrhythmic death syndrome. J Am Coll Cardiol. 2012;59:1659-60.	14.086
30	Kubben N, Voncken JW, Konings G, van Weeghel M, van den Hoogenhof MM, Gijbels M, van Erk A, Schoonderwoerd K, van den Bosch B, Dahlmans V, Calis C, Houten SM, Misteli T, Pinto YM. Post-natal myogenic and adipogenic developmental: Defects and metabolic impairment upon loss of A-type lamins. *Nucleus.* 2011;2:195-207	
31	Meder B1, Haas J, Keller A, Heid C, Just S, Borries A, Boisguerin V, Scharfenberger-Schmeer M, Stähler P, Beier M, Weichenhan D, Strom TM, Pfeufer A, Korn B, Katus HA, Rottbauer W.Targeted next-generation sequencing for the molecular genetic diagnostics of cardiomyopathies.Circ Cardiovasc Genet. 2011;4:110-22.	6.728

32	Villard E, Perret C, Gary F, Proust C, Dilanian G, Hengstenberg C, Ruppert V, Arbustini E, Wichter T, Germain M, Dubourg O, Tavazzi L, Aumont MC, DeGroote P, Fauchier L, Trochu JN, Gibelin P, Aupetit JF, Stark K, Erdmann J, Hetzer R, Roberts AM, Barton PJ, Regitz-Zagrosek V; Cardiogenics Consortium, Aslam U, Duboscq-Bidot L, Meyborg M, Maisch B, Madeira H, Waldenström A, Galve E, Cleland JG, Dorent R, Roizes G, Zeller T, Blankenberg S, Goodall AH, Cook S, Tregouet DA, Tiret L, Isnard R, Komajda M, Charron P, Cambien F. A genome-wide association study identifies two loci associated with heart failure due to dilated cardiomyopathy. *Eur Heart J*. 2011;32:1065-76.	14.097
33	Garcia-Pavia P, Syrris P, Salas C, Evans A, Mirelis JG, Cobo-Marcos M, Vilches C, Bornstein B, Segovia J, Alonso-Pulpon L, Elliott PM. Desmosomal protein gene mutations in patients with idiopathic dilated cardiomyopathy undergoing cardiac transplantation: a clinicopathological study. Heart. 2011;97:1744-52	5.014
34	Meder B, Huttner IG, Sedaghat-Hamedani F, Just S, Dahme T, Frese KS, Vogel B, Köhler D, Kloos W, Rudloff J, Marquart S, Katus HA, Rottbauer W. PINCH Proteins Regulate Cardiac Contractility by Modulating Integrin-Linked Kinase-Protein Kinase B Signaling. *Mol Cell Biol*. 2011;31:3424-35.	7.308
35	Arbustini E, Grasso M. Human "nuclear" mitochondrial cardiomyopathy a novel mouse model characterizes the disease. *JACC Cardiovasc Imaging*. 2011;4 :11-5.	6.164
36	Just S, Berger IM, Meder B, Backs J, Keller A, Marquart S, Frese K, Patzel E, Rauch GJ; Tübingen 2000 Screen Consortium, Katus HA, Rottbauer W. Protein kinase D2 controls cardiac valve formation in zebrafish by regulating histone deacetylase 5 activity. *Circulation*. 2011;124:324-34.	15.202
37	Just S, Meder B, Berger IM, Etard C, Trano N, Patzel E, Hassel D, Marquart S, Dahme T, Vogel B, Fishman MC, Katus HA, Strähle U, Rottbauer W. The myosin-interacting protein SMYD1 is essential for sarcomere organization. *J Cell Sci*. 2011;124:3127-36.	5.9
38	Diegoli M, Grasso M, Favalli V, Serio A, Gambarin FI, Klersy C, Pasotti M, Agozzino E, Scelsi L, Ferlini A, Febo O, Piccolo G, Tavazzi L, Narula J, Arbustini E. Diagnostic work-up and risk stratification in x-linked dilated cardiomyopathies caused by dystrophin defects. *J Am Coll Cardiol*. 2011;58:925-34.	14.086
39	Zaragoza MV, Brandon MC, Diegoli M, Arbustini E, Wallace DC. Mitochondrial cardiomyopathies: how to identify candidate pathogenic mutations by mitochondrial DNA sequencing, MITOMASTER and phylogeny. *Eur J Hum Genet*. 2011;19:200-7.	4.319
40	Haas J, Katus HA, Meder B. Next-generation sequencing entering the clinical arena. *Mol Cell Probes*. 2011;25:206-11.	1.873
41	Griffin JL, Atherton H, Shockcor J, Atzori L., metabolomics as a tool for cardiac research. *Nat Rev Cardiol.* 2011;8:630-43.	10.4
42	Bellazzi R, Larizza C, Gabetta M, Milani G, Bucalo M, Mulas F, Nuzzo A, Favalli V, Arbustini E. Information technology solutions to support translational research on inherited cardiomyopathies. *Stud Health Technol Inform*. 2011;169:907-11.	
43	Nuzzo A, Mulas F, Gabetta M, Arbustini E, Zupan B, Larizza C, Bellazzi R. Text Mining approaches for automated literature knowledge extraction and representation. *Stud Health Technol Inform*. 2010;160:954-8.	

44	Zaragoza MV, Fass J, Diegoli M, Lin D, Arbustini E.Mitochondrial DNA variant discovery and evaluation in human Cardiomyopathies through next-generation sequencing. *PLoS One.* 2010;5(8):e12295.	3.730
	Total	**271.174**

Other scientific products

PATENT: BIO-10917, Inserm-transfert « In vitro diagnosis method for predicting a predisposition to cardiomyopathy").

INHERITANCE website: www.inheritanceproject.eu

MOGES website: http://moges.biomeris.com

CARDIOREGISTER website: https://cardioregister.com/Pages/Main.aspx

i2b2 website for inheritance: http://i2b2inheritance.com

Wikipedia for inheritance: http://www.labmedinfo.org:8123/mediawiki/index.php/Main_Page

Alterations in cardiac DNA methylation in human dilated cardiomyopathy: data submitted to GEO (http://www.ncbi.nlm.nih.gov/geo/) , accession number GSE42510.